SPATIAL AND TEMPORAL VARIATIONS IN URBAN AIR TEMPERATURE

SPATIAL AND TEMPORAL VARIATIONS IN URBAN AIR TEMPERATURES

G. Brett Maxwell

Department of Geography Master of Science

Nocturnal variations in cooling rates and air temperatures for downtown, industrial and residential areas in Montreal and a nearby rural area were compared under calm and clear weather conditions.

A selection of sampling densities was analysed to determine their adequacy in depicting urban air temperature patterns. The heat island was formed for the most part in the early evening because of divergence of cooling rates between urban and rural areas, and then stabilized for the remainder of the night. Maximum nocturnal values occurred three to four hours after sunset, and intensity reached a limiting maximum value under ideal wind and cloud conditions. Urban morphology was shown to have a major influence on air temperatures and cooling rates were shown to vary within the urban area according to land use.

LES VARIATIONS SPATIALES ET TEMPORELLES DE LA TEMPERATURE DE L'AIR DANS LES REGIONS URBAINES

G. Brett Maxwell

Département de géographie Maîtrise ès sciences

Les variations nocturnes dans les taux de refroidissement et dans les températures de l'air pour le centre ville, les régions industrielles, résidentielles et rurales sont comparées sous des conditions atmosphériques favorables.

Afin de déterminer les variations de tempêratures urbaines un échantillon de densité doit être choisi. L'ilôt de chaleur est formé tôt dans la soirée du aux différents taux de refroidissement entre les régions urbaines et rurales puis se stabilise par la suite. Les valeurs maximales surviennent trois à quatre heures après le coucher du soleil et l'intensité parvient a une valeur maximale sous des conditions atmosphériques favorables. Nous voyons que la morphologie urbaine influence aussi les taux de refroidissement et la température de l'air selon l'utilisation de la région urbaine.

SPATIAL AND TEMPORAL VARIATIONS IN URBAN AIR TEMPERATURES

G. Brett Maxwell

A thesis submitted to the Faculty of Graduate Studies and Research, McGill University, in partial fulfillment of the requirements for the degree of Master of Science.

Department of Geography,
McGill University,
Montreal, Quebec.

July, 1971

© G. Brett Maxwell 1971

ACKNOWLEDGEMENTS

The research for this thesis would not have been possible without the assistance of Miss Patricia Stark and Mr. Steve Barg who shared the driving of the survey automobile with the author on the nights of observations. Appreciation is extended to Mr. Dave Yap for the many constructive discussions on the subject matter of the thesis, and to Miss Sheila MacBain for her valuable advice and perspective broadening discussions during the last stages of thesis preparation. I would also like to express special thanks to Mlle Viviane Côté for inspiration and assistance throughout the preparation of the thesis.

Final preparation of the manuscript would have been impossible without the efforts put forth by Miss Barbara Cooper, who typed the thesis, and Mr. Jim Bogart who prepared some of the diagrams.

Finally, I would like to express my appreciation to Dr. T.R. Oke who supervised the preparation of this thesis.

This study is part of a project funded by the National Research Council of Canada, and the Canadian Meteorological Service, Ministry of Transport, under operating grants to Dr. T.R. Oke.

TABLE OF CONTENTS

LIST OF TABLES

LIST OF FIGURES

CHAPTER I

INTRODUCTION

Current knowledge of urban air temperatures is mainly based on descriptive case studies which show that air temperatures in an urban area are commonly several degrees warmer than those in a nearby rural or suburban area. This warmth depends on many factors, primarily those which are uniquely urban such as the physical nature of urban surfaces, air pollution, artificial heating and large, dense populations. There are also more general meteorological factors, such as wind and cloud, which act as controls on the effects of the previous factors.

The influence of the meteorological factors (Sundborg 1951, Chandler 1965) and the effects of topography (Middleton and Millar 1936, Chandler 1962a) are quite well documented. Artificial heat production has been evaluated for a number of cities, (Summers 1964, Garnett and Bach 1965, Bornstein 1968, Bach 1970) and recent studies have investigated the relationship between air pollution and air temperatures, especially the vertical distribution of temperature (Bornstein 1968, Yap 1969, Oke and East 1971). Little attention has been focussed, however, on changes between urban and rural locations that occur because of the different physical surfaces of the two environments. No systematic study has yet been published evaluating the adequacy of observational sampling densities used in previous descriptive studies.

These spatial aspects of urban air temperature variations are investigated in this thesis from observational data gathered in Montreal. In addition, there has been little study of temporal variations of urban air temperatures and urban-rural temperature differences, and this aspect is also investigated.

1. The Urban Heat Island

The term 'urban heat island' refers to the characteristic warmth or temperature excess of an urban area compared to an adjacent rural or suburban area. It draws the climatic analogy of the city appearing as a land mass in the sea of the surrounding countryside, based on the contrasting heat responses of the land/water and urban/rural surfaces (Oke 1969).

A useful framework within which to study these heat responses is that of the heat balance, which provides an assessment of the utilization of available energy. The rural heat balance may be stated as:

$$Rn = H + LE + G$$

and for the urban area:

$$Rn + F = H + LE + G$$

where, Rn is the net all wave radiation

H is convective sensible heat transfer

LE is latent heat transfer

G is soil heat storage or heat storage in the urban surface materials

F is artificial heat generated by combustion and metabolic processes in the urban area.

The heat island is a dynamic phenomenon, responding to changes in both the urban and rural heat balances which themselves vary with time. It is therefore more useful to think in terms of the rate of change of temperature ($\Delta T/\Delta t$) than actual air temperatures. $\Delta T/\Delta t$ is a function, firstly, of the available energy (Rn, F) and secondly, the partitioning of that energy among the terms H, LE, and G. Different rates of energy exchange in urban and rural areas will determine urban and rural temperatures and thus the magnitude of the heat island intensity (ΔT_{u-r}).

The influence of an urban area on cooling rates and air temperatures, as expressed by the effects on individual heat balance terms, is outlined briefly in the following paragraphs. No attempt is made to assign numerical values to the terms as little is known about the relative magnitudes of the individual terms (Rn, F, H, LE, G) of the urban heat balance equation (Munn 1966, Lowry 1967). Only the nocturnal situation is considered because the heat island is generally agreed to be most pronounced at night, and the radiative exchange is somewhat simplified due to the absence of solar radiation.

Cooling rates: In general, one might expect nocturnal cooling rates to be less in an urban area than those in a rural area. The large amount of heat stored (G) in the urban fabric will be released during the night tending to oppose the radiative cooling process; and thus giving the city thermal inertia. Artificial heat generation (F) is likely to enhance this thermal inertia, especially during the heating season when space heating energy releases increase at night as temperatures begin dropping.

Temperature: At night urban air temperatures tend to be warmer for four main reasons. Firstly because of the higher heat capacities of urban materials and the dense physical structure of the urban area, the urban area should tend to absorb more heat during the day than the rural area, permitting the storage term (G) to assume a much larger value and thus provide a greater quantity of heat to dissipate at night. Secondly, artificial heat (F) will contribute to urban warming by radiation, and conduction through the walls of buildings and through the effluent from automobile exhausts and chimneys. Chimney effluent is unlikely to contribute directly towards energy available at street level, but motor vehicle exhaust is likely to warm the air in the lowest few metres. Thirdly, convective sensible heat transfer (H) may be increased because of the large energy inputs at night from G and F; however Oke (1969) is of the opinion that H may be reduced as a result of stagnation between the roughness elements of the urban structure. Latent heat transfer (LE) may also be reduced because of the small number of evaporative surfaces in an urban area. Little is known about the partitioning of available energy between H and LE in the urban environment. Fourthly, the urban area (especially the Central Business District (CBD)) may lose less heat by long-wave radiation to its relatively warm and polluted surrounding environment, than the rural area which is usually well exposed to a cool, clear night-time sky. This decrease in the effective outgoing radiation (I), which is the net radiation (Rn) at night, may appear contradictory as long-wave radiation from the urban fabric ($I\uparrow$) is likely to be greater in the warmer urban area. If I is indeed less from the city it will be as a result of increased

atmospheric counter radiation ($I\downarrow$) from the warm and polluted urban air.[1] This may in fact be a minor contributor to urban warming as it is possible that the increases in $I\uparrow$ and $I\downarrow$ could cancel each other.[2]

a) Urban Morphology

The terms 'fabric' and 'structure' have been introduced and their usage follows that of Oke (1969). 'Urban fabric' refers to the bricks, concrete, steel, asphalt and glass that form a drier, less pervious, and more rigid surface in the urban area than in the countryside. 'Urban structure' refers to the configuration of buildings resulting in a much larger effective surface area, and rougher surface than the rural countryside of equivalent plan size. This term also encompasses the changes in continuity, height and function of buildings, along with the irregular size and spacing of open and undeveloped areas. These two concepts together define the term 'urban morphology'.

Previous authors have stated that urban morphology has a major influence on urban air temperatures. Sundborg (1950) comments that changes in the surface configuration of a compact city are sufficient to produce a modification of the climatological elements, but does not attempt to

---

1. It has recently been shown that $I\downarrow$ increases some 5% from rural to urban areas in Montreal (Fuggle 1971), and also that this increase is due to the increased warmth of the urban atmosphere rather than a change in the radiative properties of the atmosphere attributable to pollution (Oke and Fuggle 1971).

2. Oke and Fuggle (1971) have also shown that increased long wave radiation from the urban fabric ($I\uparrow$) and the increased urban counter radiation ($I\downarrow$) do offset each other, with the result that the effective outgoing radiation (I) is little different between urban and rural areas at night. It thus appears that the net radiative exchange contributes little to urban warming, but changes in the component fluxes are important.

isolate and evaluate these effects. Duckworth and Sandberg (1954) state, on the basis of isotherm maps, that the most important single factor in increasing the temperature in an urban area appears to be the morphology of the city - the tall concrete and brick buildings between cement and asphalt pavements. They also claim that, compared to soil, the capacity of urban building materials to release stored heat can account for more than half of most observed nocturnal temperature differences. They do not explain how this figure was derived. Chandler (1962a, 1965) is of the opinion that local urban morphologies, in particular the size of open areas and the continuity and height of buildings, dominate over large scale considerations on calm nights. This is based on analysis of temperature profiles across London, England. Ludwig and Kealoha (1968) provide a comprehensive, qualitative evaluation of the effects of urban morphology on the processes affecting air temperature. In summary, however, there is still little observational evidence to verify or evaluate the influence of urban morphology on air temperatures, and it is one of the aims of this thesis to provide such evidence.

b) Heat Island Descriptive Parameters

Air temperatures are usually warmest near the centre of the most densely built-up part of an urban area (heat island core), then decrease gradually towards the edge of the built-up area. Temperatures then tend to drop sharply, forming a 'cliff' of temperature near the boundary of a built-up area with its surrounding countryside. The two descriptive parameters usually applied to the heat island arise from the above characteristics.

Firstly, there is the areal size or spatial extent, that is, the total area enclosed by the heat island. Sundborg (1951) noted that there is a strong temperature gradient, with temperature decreasing outwards from the urban area, at the boundary between populated and unpopulated sectors in Uppsala, Sweden. This strong gradient has also been noted by Duckworth and Sandberg (1954) in San Francisco; Chandler (1965) in London, England; Daniels (1965) in Edmonton, Alberta; Oke and Hannell (1970) in Hamilton, Ontario; and Oke (1968) in Montreal, Quebec, suggesting that the area of the heat island is closely related to the extent of the built-up area.

Secondly, there is the heat island intensity, which is the instantaneous difference of temperature between the urban area and the surrounding rural area. Many working definitions have appeared in the literature, but that employed by Duckworth and Sandberg (1954) appears to be the most suitable, and is employed here. Heat island intensity (ΔT_{u-r}) therefore is defined as the difference between the maximum and minimum observed temperatures in the traversed area, after all readings have been reduced to a common time. The intensity is usually greatest on calm, clear nights, and representative values of ΔT_{u-r} at night under favourable weather conditions (light winds and scattered or no cloud) for several cities are given in Table 1. The period of observation is not the same in all cases but the figures in Table 1 give an idea of the magnitude of nocturnal intensities.

TABLE 1

Representative Nocturnal Values of Heat Island Intensity

City	Population	ΔT_{u-r} (°C)	Period of Observation	Author
San Francisco, California	784,000	6 - 7	Year	Duckworth and Sandberg (1954)
Hamilton, Ontario	300,000	5 - 6	Fall/Winter	Oke and Hannell (1970)
San Jose, California	101,000	4 - 5	Year	Duckworth and Sandberg (1954)
Edmonton, Alberta	340,000	3	Winter/Summer	Daniels (1965)
Palo Alto, California	33,000	2 - 4	Year	Duckworth and Sandberg (1954)

Extreme nocturnal ΔT_{u-r} values of over 10°C have been reported in several studies (Middleton and Millar 1936, Duckworth and Sandberg 1954, Daniels 1965). A portion of these extreme differences is probably attributable to the topography and other non-urban controls of the cities concerned, but the major portion of the observed heat island is likely to be urban induced. Unfavourable weather conditions (moderate to strong winds and overcast skies) reduce the heat island intensity to a low value. In fact, there appears to be a critical value of wind speed, above which ΔT_{u-r} is reduced to an insignificant value (less than 1°C) (Oke and Hannell 1970). The critical wind speed is a function of city size.

This section has only presented those basic aspects of the heat island that are pertinent to the research at hand, and the reader is referred to a comprehensive survey of recent literature by Peterson (1969) and extensive bibliographies gathered by Chandler (1965, 1970) and Ludwig and Kealoha (1968) for a detailed examination of all aspects of the urban heat island.

2. Topics for Investigation

a) Sampling Density

The decision concerning the requisite number of observation points to adequately depict spatial variation of air temperature is important to any study of the urban heat island.

Previous studies have employed varying numbers of observation points per unit area, the actual number being mainly dictated by limitations of equipment and personnel. These limitations are usually most severe if fixed observation stations are employed. Chandler (1965) established a network of up to 60 fixed climatological stations in London, England to supplement the 18 synoptic stations. This, however, resulted in a sparse sampling density of approximately 1 point 20 km^{-2} or 0.05 point km^{-2}.

The traverse technique, using automobiles or other means of transportation to move a sensor through an area, permits a greater number of observation points but also has limitations. A traverse is usually limited to two or three hours duration as that is the longest period during which one can reasonably expect an approximately linear change in ambient temperature with time. A linear change is necessary to enable

the temperatures observed at various times along the route to be simply corrected to a common time for comparative analysis.

One of the highest sampling densities reported is approximately 20 points km^{-2} for Palo Alto, California, and the authors comment that this density gives quite thorough coverage (Duckworth and Sandberg 1954). One point km^{-2} is the lowest density reported in studies utilizing the traverse technique, and would seem to be a reasonable minimum value to enable meaningful analysis to be carried out. This density has been reported in studies of Edmonton, Alberta (Daniels 1965); Montreal, Quebec (Oke 1969); and Sheffield, England (Garnett and Bach 1966). These are computed densities rounded to the nearest whole number, and do not imply that every square kilometer will contain the given number of points. In fact, it is quite possible that different densities were employed in various parts of the city.

A comparative study of various sampling densities in a particular urban area and the adequacy of each to depict the air temperature pattern over the area has not been published to date, and is presented in this thesis.

b) Diurnal Variation of Heat Island Intensity

The few studies dealing with the diurnal variation of ΔT_{u-r} have used different sources for air temperature data. Daniels (1965) showed that this can lead to large differences in intensity. Daniels presents average intensity values for summer and winter from a series of systematic automobile traverses between the city of Edmonton, Alberta, and the surrounding countryside. He also reports intensity values

derived by comparing temperatures at the downtown Industrial Airport with those at the International Airport 19 km south of the city. Daniels concludes, from traverse data, that the greatest city/country air temperature difference occurred in the early morning (0300 to 0600[1] in winter, and 0000 to 0300 in summer), and the smallest difference occurred in the late afternoon (1400 to 1600). The airport intensities on the other hand appear to underestimate ΔT_{u-r}.

Other authors have compared city/country differences from maximum and minimum screen temperature data and find that generally ΔT_{u-r} is greatest from the minimum temperature data (Kraus 1945, Landsberg 1956, Chandler 1962b). The intensities derived by these authors are probably underestimates of the actual intensity as defined in section 1, for two reasons. Firstly, the maximum and minimum temperatures at the city and country stations may not occur at the same time. Maximum temperatures may occur hours apart (Ludwig 1967), thus the comparison is not being made at a common time. Secondly, the stations used may not typify the areas they are supposed to represent. The city maximum used may not have been taken at the warmest part of the CBD, and the airport temperatures have often been taken to represent country temperatures. Ludwig and Kealoha (1968) state that daytime airport temperatures are actually fairly representative of CBD temperatures in an area of tall buildings.

---

1. All times in this thesis are local standard time.

The only general conclusion that can be drawn from the above literature is that heat island intensity is greatest during the night-time hours and least during the day. There is a distinct lack of detailed knowledge of daytime and nocturnal variations in heat island intensity, and this thesis investigates nocturnal variations in detail.

c) Warming/Cooling Rates

Previous research on the urban heat island has not considered the dynamic aspect of this phenomenon. Little detailed attention has been given to the diurnal variation of the heat island as has been shown in b) above, and little research has been published on variations in the rate of change of air temperatures - the warming or cooling rates ($\Delta T/\Delta t$). Differences and variations in these cooling rates might help to explain the growth and decay dynamics of the urban heat island.

The thermal inertia of the city, coupled with the contribution of artificial heating must lead to a different rate of change of temperature to that in a rural area, but the actual rates of change of air temperature have not been compared. In addition, it is likely that $\Delta T/\Delta t$ may vary as the surface morphology of the urban area changes. It is not known if diurnal variation of $\Delta T/\Delta t$ measured at one location in one morphological zone, is typical of variations of $\Delta T/\Delta t$ in other zones of differing but internally consistent morphology. Such zones can be defined in terms of the division of the urban area into functional zones such as Central Business District (CBD), industrial, or residential zones. This thesis compares urban and rural $\Delta T/\Delta t$ and relates the growth and

decay dynamics of ΔT_{u-r} to these rates.

3. Scope and Limitations

The topics outlined in section 2 were investigated by studying nocturnal variations in air temperatures in Montreal. Observations were limited to night times for two reasons. Firstly, it is at night that the urban heat island is most pronounced, and the effects of the factors that control it should then be most discernable. Secondly, greater pollution potential exists at night - with relatively stable air, light winds, and often an elevated inversion that 'caps' the vertical dispersion of pollutants. An understanding of the horizontal variation of urban air temperatures for this period of the day could contribute to a better understanding of the horizontal dispersion of pollutants.

Detailed observations of air temperatures are confined to the City of Montreal and its immediate surroundings, and thus may only be directly applicable to that area.

4. Summary of Objectives

The objective of this thesis is to contribute toward knowledge of the spatial and temporal variations in air temperatures that characterize the urban heat island. To this end, the following aims were pursued:

i) to evaluate the effects of sampling density in the study of urban air temperature variations;

ii) to obtain detailed observations of the nocturnal variations in the intensity of the heat island ΔT_{u-r}, through a comparison of urban

and rural air temperatures and cooling rates ($\Delta T/\Delta t$);

iii) to obtain observational evidence of the effects of intra-urban changes in morphology on air temperatures and cooling rates.

CHAPTER II

INSTRUMENTATION

The detailed observations of air temperatures required to fulfill the aims of this thesis necessitate the use of an accurate, fast response sensor coupled with a rugged recording device that can easily be installed in an automobile. The following requirements were considered essential in a sensor-recorder assembly:

i) Accuracy - an overall accuracy of approximately $\pm 0.25^{o}C$;

ii) Response time - a response time of < 1 sec;

iii) Recording - a continuous record of temperature be produced so that features appearing between pre-determined points may be studied;

iv) Event marker - an event marker be included to make precise location of check points possible;

v) Ease of operation - the sensor-recorder assembly be operable by one man while driving;

vi) Maintenance - sensor-recorder assembly be as simple as possible to decrease the chances of breakdown and the need for maintenance.

1. Sensor and Recorder

The recording instrument chosen was a single-channel Rustrak 115 volt AC strip chart recorder, recording on a 5 cm wide chart (Figure 1) (Gulton Industries Inc., Rustrak Instrument Division,

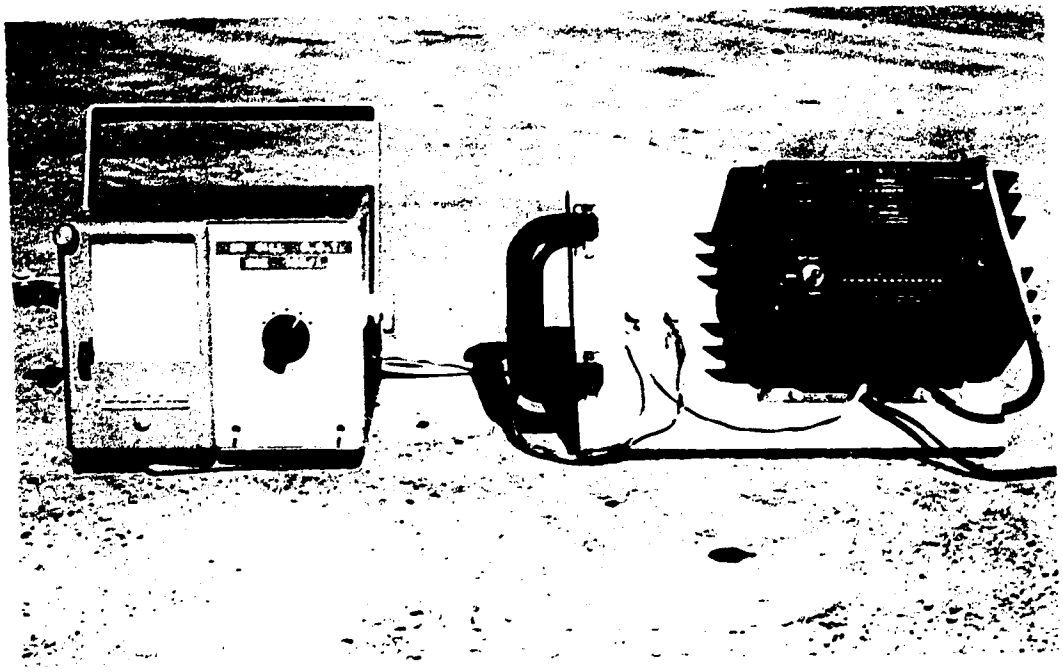

Figure 1: Air temperature recorder (left), and DC/AC inverter (right).

Figure 1: Air temperature recorder (left), and DC/AC inverter (right).

Manchester, New Hampshire - Model 133). This model is designed for use with a thermistor temperature sensor, and is built to withstand harsh environments. It is equipped with a DC galvanometer designed to withstand the shocks to be expected from use in a moving vehicle.

The recorder is direct reading, with the scale calibrated in (^{o}C), and can be used over a total temperature range of from -30 ^{o}C to +33 ^{o}C. The full scale range of the recorder is 15 ^{o}C and there are five separate ranges each overlapping adjacent ranges by 3 ^{o}C as follows: -30 to - 15 ^{o}C, -18 to -3 ^{o}C, -6 to +9 ^{o}C, +6 to +21 ^{o}C, +18 to +33 ^{o}C. Switching is accomplished by a five-position switch on the front of the recorder. Temperature is recorded every four seconds by impaction of a stylus on the pressure sensitive paper. The chart speed is adjustable and the most satisfactory speed for this study was found to be 15 cm hr^{-1}. The recorder is equipped with an event marker. The window over the chart opens to enable notes to be written directly on the chart.

The sensor used in this study was a thermistor element in the form of a flat disk (diameter 1 cm, thickness 0.3 cm), mounted on the end of a 10 cm probe (Gulton Industries Inc., Rustrak Instrument Division, Manchester, New Hampshire - Model 1333) (Figure 2a). The thermistor has a time constant (time required to respond to 63.2% or $1 - e^{-1}$ of a step change in environmental temperature) of 0.8 seconds. The response characteristics were tested and found to be linear.

Figure 2(a): Sensor housing with radiation shield removed to show sensor.

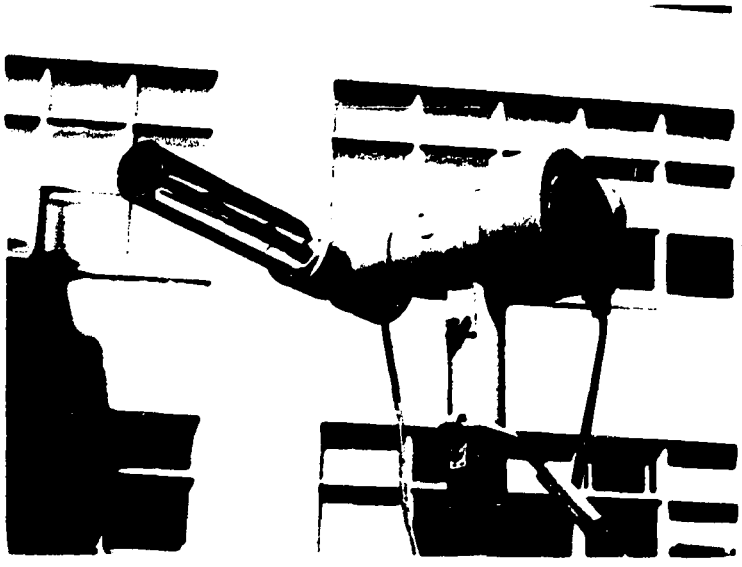

Figure 2(b): Sensor housing with radiation shield in place. Ventilation fan is on the right.

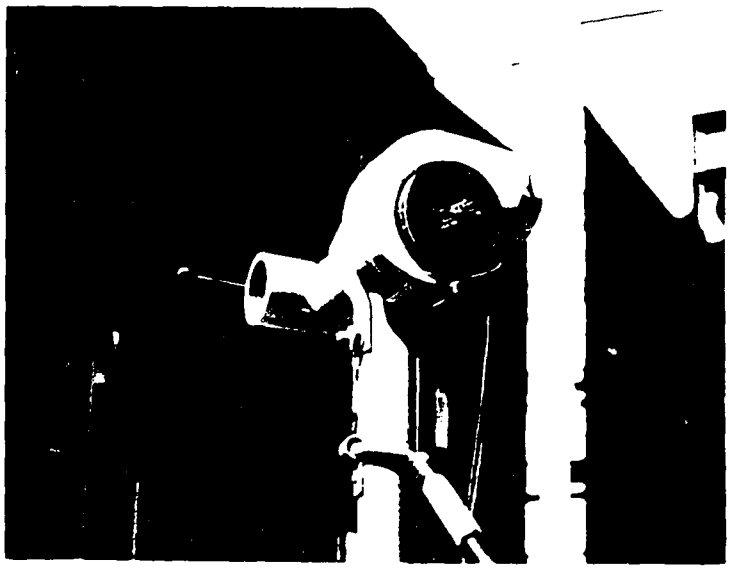

The sensor was installed in a ventilated radiation shield constructed from polyvinyl chloride (PVC) tubing and fittings (Figure 2b). Ventilation is necessary to ensure that the environmental air is drawn past and not permitted to stagnate around the sensor, regardless of automobile speed. Shielding is required to prevent the sensor from being cooled or warmed directly by radiation from any source. PVC tubing was chosen because of its light weight and low thermal conductivity (0.345×10^{-3} cal $cm^{-1} sec^{-1}$ $^{o}C^{-1}$). The radiation shield was 15 cm in length and was covered with highly-reflective Mylar tape to offset solar heating, and the inside of the shield was left the dark grey of the tubing. The thermistor was supported by inserting the probe through a rubber stopper which in turn was inserted in the back of the housing. Ventilation was achieved by a small 115 volt AC, 60 Hz fan (Rotron Manufacturing Company, Woodstock, New York - Model NTH2), drawing air past the sensor at approximately 3 m sec^{-1}.

The 115 volt AC 60 Hz power necessary to operate the recorder and the fan was provided by a DC/AC inverter (Heath Company, Benton Harbour, Michigan - Model MP-10) operating from the automobile 12 volt DC battery. A 12 volt DC power connection was provided at the input side of the inverter for the event marker (Figure 3).

The recorder accuracy is $\pm 2\%$ of the full scale span of the recorder between 0 ^{o}C and 100 ^{o}C. This gives an absolute accuracy of ± 0.3 ^{o}C including the ± 0.1 ^{o}C readability of the chart paper. A built-in calibration check is provided on the recorder. To verify this calibration, laboratory comparisons were conducted with an NPL standard

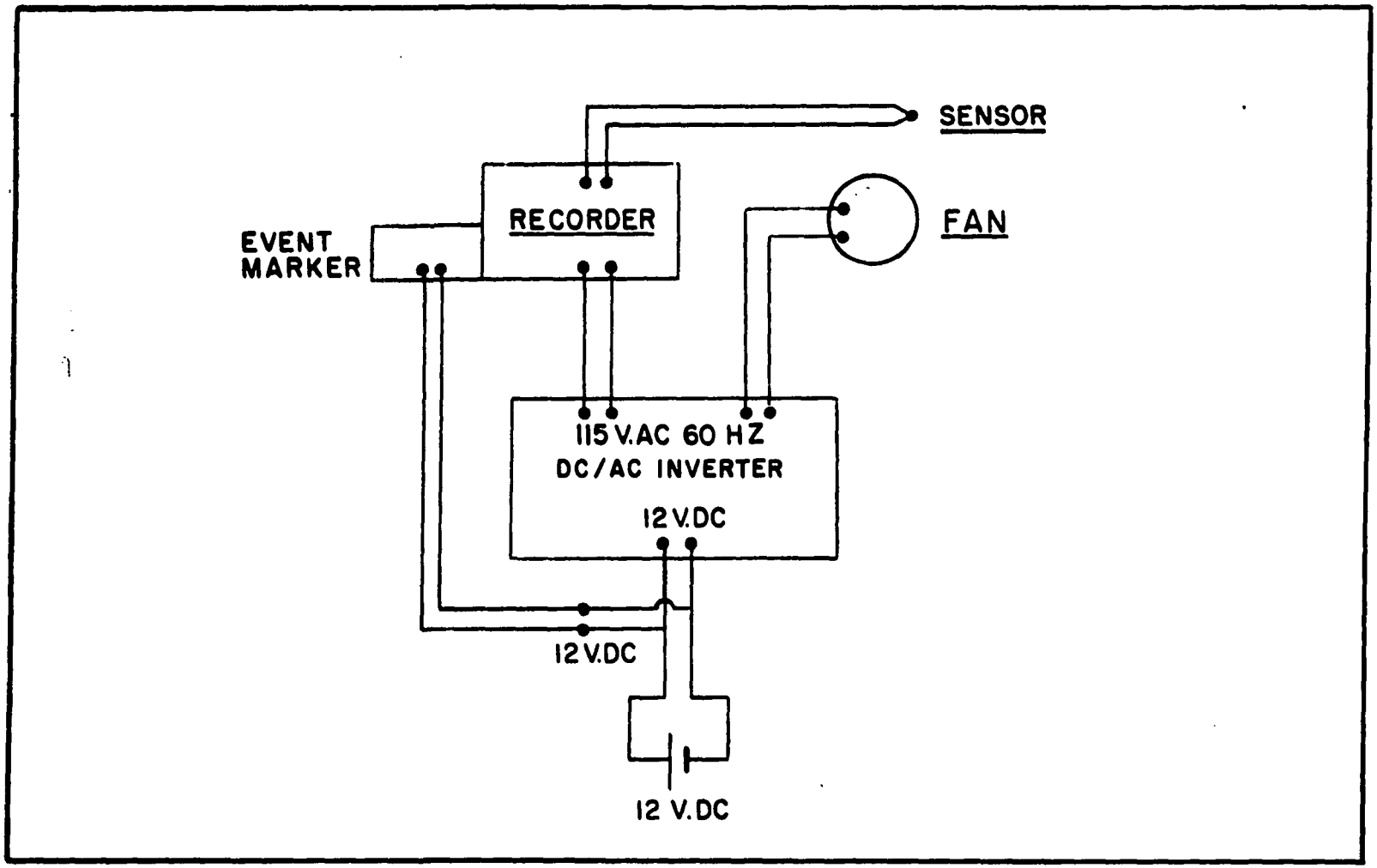

Figure 3: Circuit Diagram

mercury-in-glass thermometer. The mean deviation of the system for 42 comparisons between -6 °C and +33 °C was +0.1 °C, and no deviation exceeded ±0.3 °C.

Tests were conducted to evaluate the effects of dynamic warming of the sensor at high automobile speeds, and it was found that within the limits of accuracy of the recorder, there was no dynamic warming up to a speed of 83 km hr^{-1}.

2. Mounting and Installation

The sensor housing was mounted on a PVC mast on the front bumper of the survey car, at a height of 2 m above the road surface (Figure 4). The 2 m height was chosen for four reasons. Firstly, it is the height recommended by the World Meteorological Organization for synoptic observations, and is close to that used by most weather services. Secondly, it removes the sensor from the direct effects of automobile exhausts. Thirdly, this height has been used by previous researchers (Duckworth and Sandberg 1954 , Daniels 1965 , Ludwig and Kealoha 1968), thus enabling a direct comparison to be made between the results of this study and those of other investigators. Fourthly, the lapse rate at this height is usually small enough so that mixing does not cause appreciable warming or cooling according to Ludwig (1969).

It was thought that the 2 m front bumper mounting would eliminate the possibility of heating of the sensor by the engine of the survey car, and of any other influences from the survey car itself. This was confirmed by tests conducted with sensors mounted on the mast at 2.0 m, 1.5 m, 1.0 m, 0.8 m (level of the car hood), and 0.5 m above

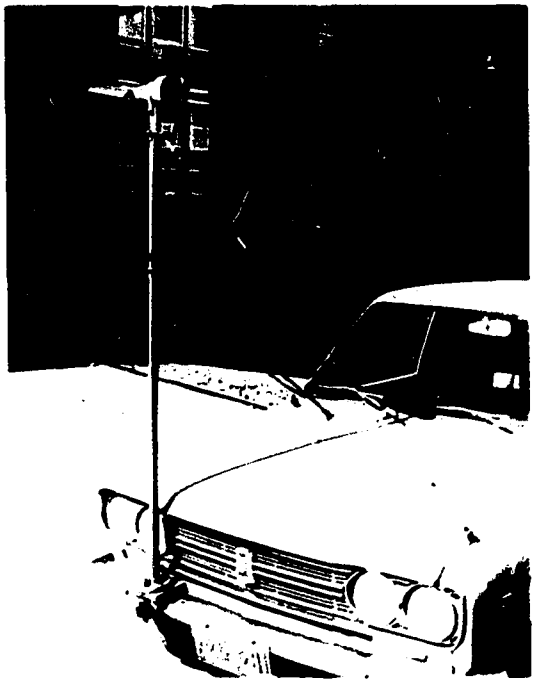

Figure 4: Mast arrangement and survey automobile.

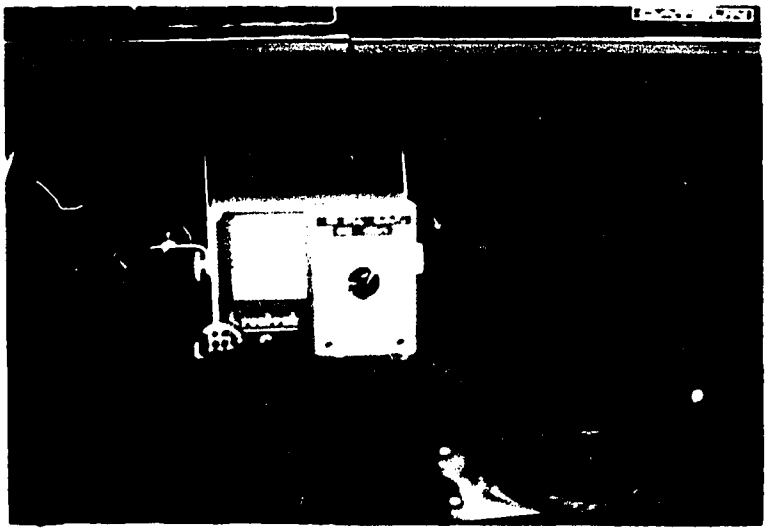

Figure 5: Installation of recorder and inverter inside car.

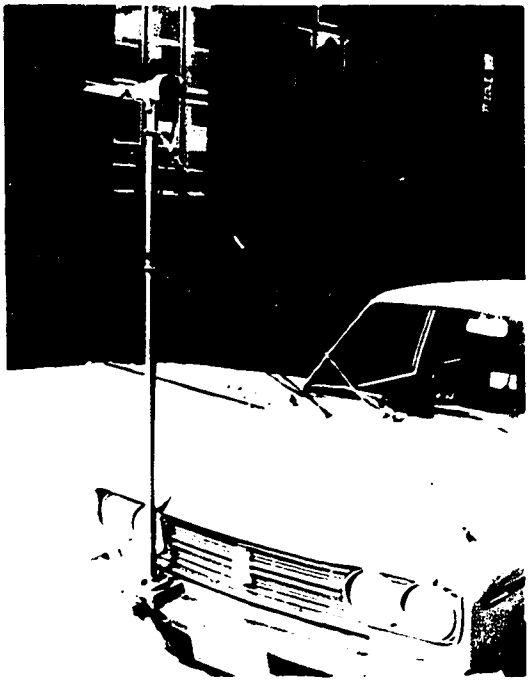

Figure 4: Mast arrangement and survey automobile.

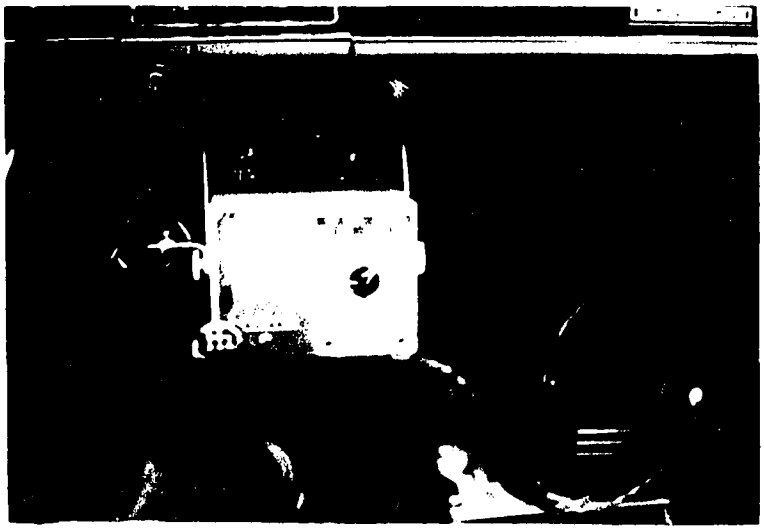

Figure 5: Installation of recorder and inverter inside car.

the road surface. With the automobile in motion at 50 km hr^{-1} there was no difference within the limits of accuracy of the instrument, in temperature between the 2 m height and any of the others. However, when the car was stopped, the temperature at the two lowest levels (0.8 and 0.5 m) increased markedly. Therefore a sensor mounted below 1 m could lead to major errors in measurement in stop-and-go city traverses. A sensor mounted on the mast between 1.0 m and 2.0 m could have been used with equal confidence.

The equipment was designed to be installed without making any permanent alterations to the automobile, and to be mounted and dismounted with a minimum of time and effort. The mast fitted into a bracket bolted onto the front bumper and was supported by two solid aluminum rods which hooked onto the hood of the car (Figure 4). The leads from the thermistor and the fan were brought into the car through the gap between the door and the frame. The inverter was connected to the cigarette lighter socket, and the recorder clamped under the dashboard (Figure 5). The entire system could be installed or removed in 10 min.

This sensing/recording system was found to be most reliable and efficient, operating without trouble in all weather conditions.

CHAPTER III

FIELD OPERATIONS

Previous urban heat island studies have employed two main methods of air temperature observation. One method is to establish a network of fixed stations equipped with standardized thermometers, throughout the urban area as was done by Chandler (1965) for London, England (60 stations) and Lindquist (1968) for Lund, Sweden (9 stations with hygrothermographs). Major problems with this method are, the difficulty of obtaining the required number of reliable observers to man the stations; standardization of thermometers; the cost of duplicating the instruments needed; and the resulting small number of observation points.

The second method is the traverse technique, using automobiles or other means of transportation to move a sensor through the urban area. The sensor may be an Assmann psychrometer (Sekiguti 1964a, Oke and Hannell 1970), but more commonly it is an electrical sensor that is either read manually at preselected observation points (Duckworth and Sandberg 1954), or records continuously (Chandler 1962a, Ludwig 1967). Temperatures obtained in this manner must be corrected for the change in ambient air temperature during the time of the traverse, before analysis is attempted. The correction is simple if the change in ambient temperature is linear during the time interval of the traverse, effectively limiting traverse periods to those times of day when one can reasonably expect an approximately linear change in ambient temperature.

The traverse technique was determined to be the most suitable method of observation for the objectives of this thesis.

1. Island of Montreal and Environs

The City of Montreal is situated on a large island of the same name at the junction of the Ottawa and St. Lawrence rivers (Figure 6). The city itself covers the middle third of the island, centred on Mount Royal (elevation 231 m above mean sea level). Large areas of the remainder of the island are built up for residential or industrial use under separate city or town governments. This suburban development extends off the island to what is referred to as the South Shore, although it is actually to the east; and to a lesser extent to the northwest onto Ile Jesus. The broad St. Lawrence valley, featureless except for the Monteregion hills of which Mount Royal is one, extends in a northeast-southwest direction and is about 100 - 150 km wide.

The CBD of the City of Montreal is immediately east of Mount Royal on the first (approximately 30 m above mean sea level) of the two terraces that mark the ascent from the river to the mountain (Figure 7). North of the mountain is a dense residential area with incursions of commercial and industrial activity. Residential areas to the west and southwest are less dense, and include commercial activity along the main streets. Those west of Montreal International Airport at Dorval, and north of the dense residential area referred to above are contemporary suburban developments. Industry is widely dispersed, mainly along the river and in industrial parks. The greatest industrial concentration is the oil refineries in Pointe aux Trembles.

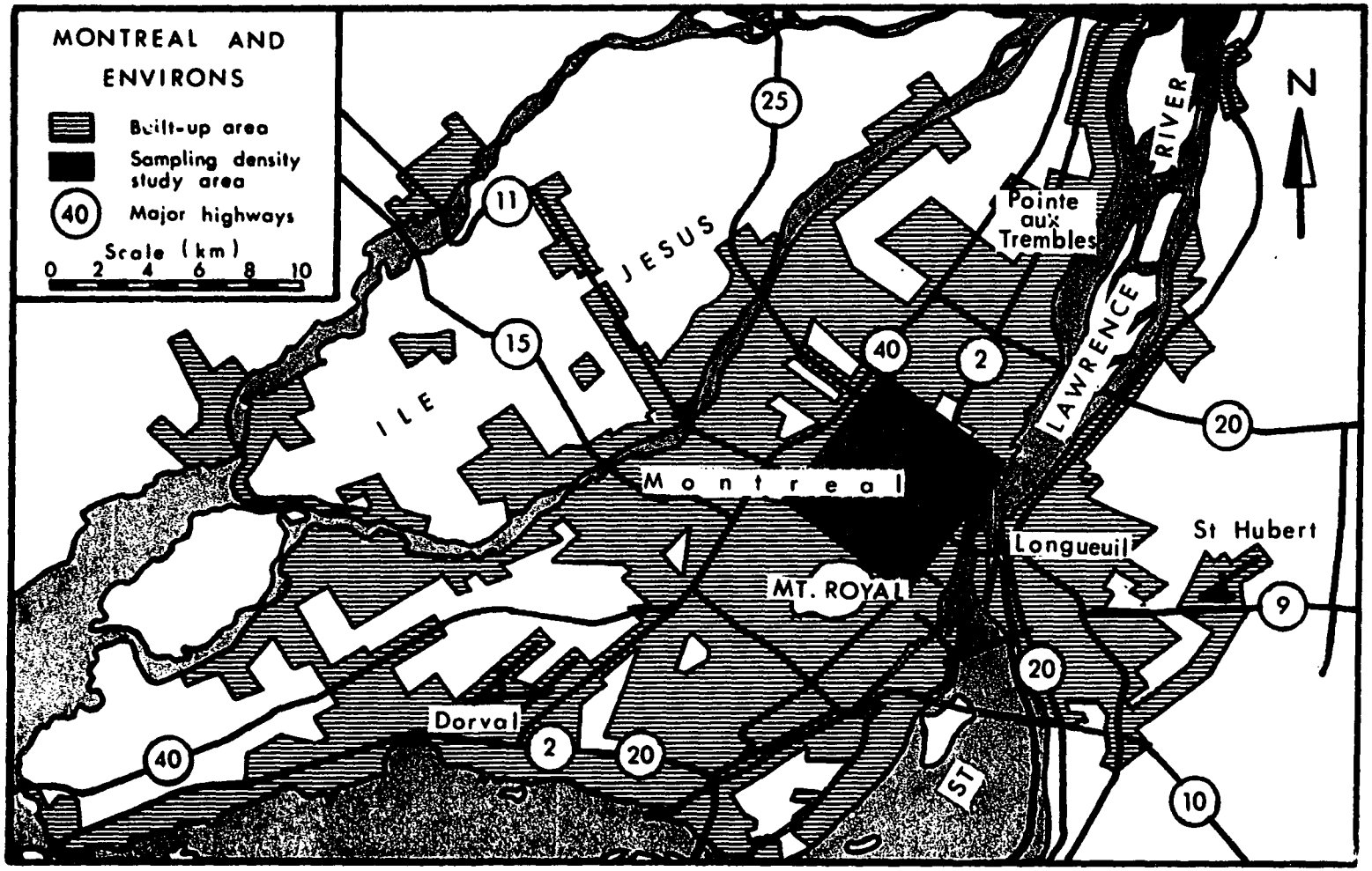

Figure 6: Location map of Montreal

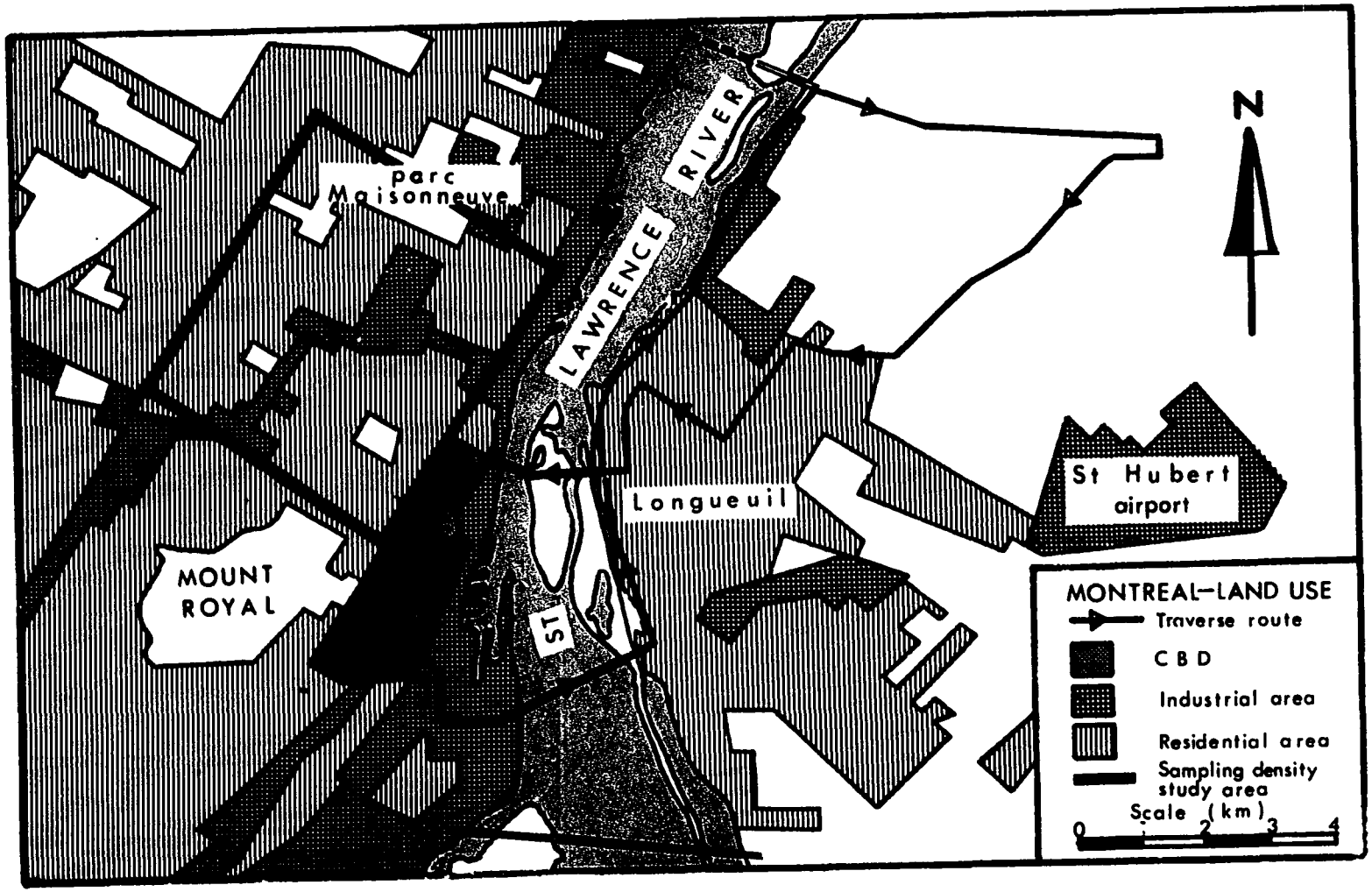

Figure 7: Cooling rate traverse route showing the CBD, industrial, residential and rural areas studied. The sampling density study areas is also shown.

Population of the City of Montreal itself is over 1,200,000 and that of the metropolitan area, including the Island of Montreal, Ile Jesus and the South Shore municipalities is over 2,300,000 (Dominion Bureau of Statistics, 1966 Census).

2. Selection of Areas for Observations

In order to evaluate the effects of intra-urban changes in morphology on air temperature and cooling rates it was necessary to delimit areas of differing morphology within the urban area. This was done on the basis of the dominant land use, assuming that the morphology within each land use area is relatively consistent. Examples of CBD, industrial, residential classifications were chosen, and are shown in Figure 7. Other factors were also considered in choosing the above areas. Firstly, the chosen areas had to be located in such a way that a closed traverse could be constructed which incorporated each of these intra-urban classifications and a rural area, and which could be completed within one hour. The rural area had to be included for the study of heat island intensity ΔT_{u-r}, and to provide a comparative rural cooling rate. Secondly, little topographic variation within each area was desirable.

'Rural' is defined here as either farmland or undeveloped land in its natural state, with the additional condition that it is not in close proximity to densely urbanized areas such as those above. The most suitable rural area was found to be the region southeast of the city core on the South Shore of the St. Lawrence, north of the St. Hubert Airport (Figure 7), with an elevation of 30 m above mean sea level. This

is a dairy farming area with no urban encroachment except the occasional house or farmstead along the roads.

The area chosen for the analysis of sampling density had to be a large area with uniform land use, little topographic variation, and easily accessible along a regular grid of streets. The most suitable area was found to be the dense residential area immediately north of Mount Royal bounded by St. Laurent, Sherbrooke, Pie IX and Belanger streets (Figure 8). This area, of approximately 15.8 km^2, is mainly residential with three or four storey flats and apartment buildings, broken by a distinct band of industrial activity along the C.P. Rail tracks, and well defined incursions of commercial activity along the main streets. The land surface slopes gradually upwards to the north-west from an elevation of 46 m at Sherbrooke street to an elevation of 58 m at Belanger.

3. Traverse Procedures

a) Cooling Rates and Heat Island Intensity

The final route for this part of the observations was 44 km long and passed through the CBD, industrial area, residential suburb, and rural section of the South Shore selected above; and is shown in Figure 7.

To achieve the required cooling rate period the route was repeated every hour. Driving speed was kept below 67 km hr^{-1} in the sections of the route that were of immediate interest (the areas designated as CBD, residential, industrial, and rural) and the distance between these areas was covered as quickly as possible. With little

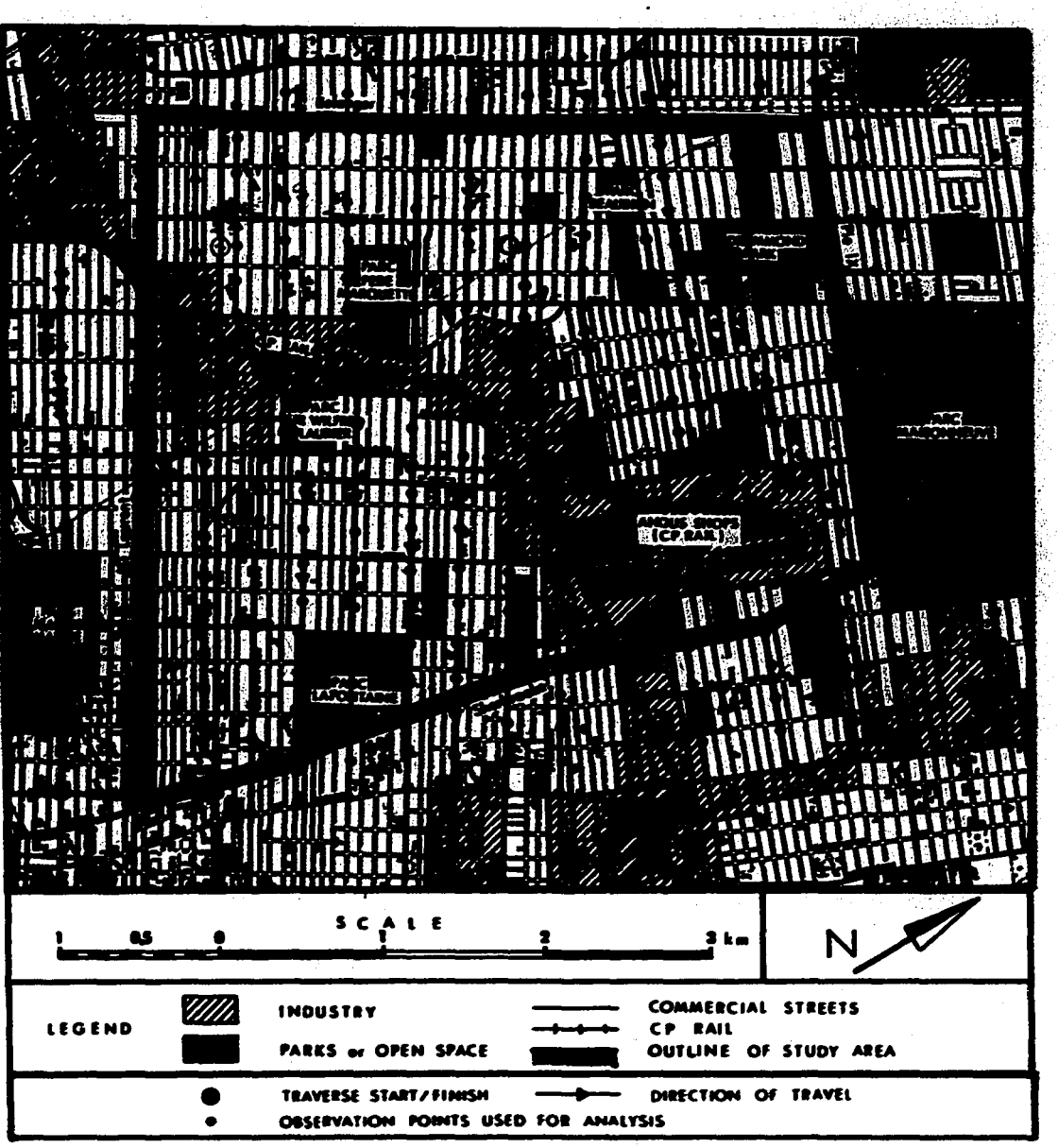

Figure 8a: Sampling density study area

Figure 8b: Sampling density traverse route

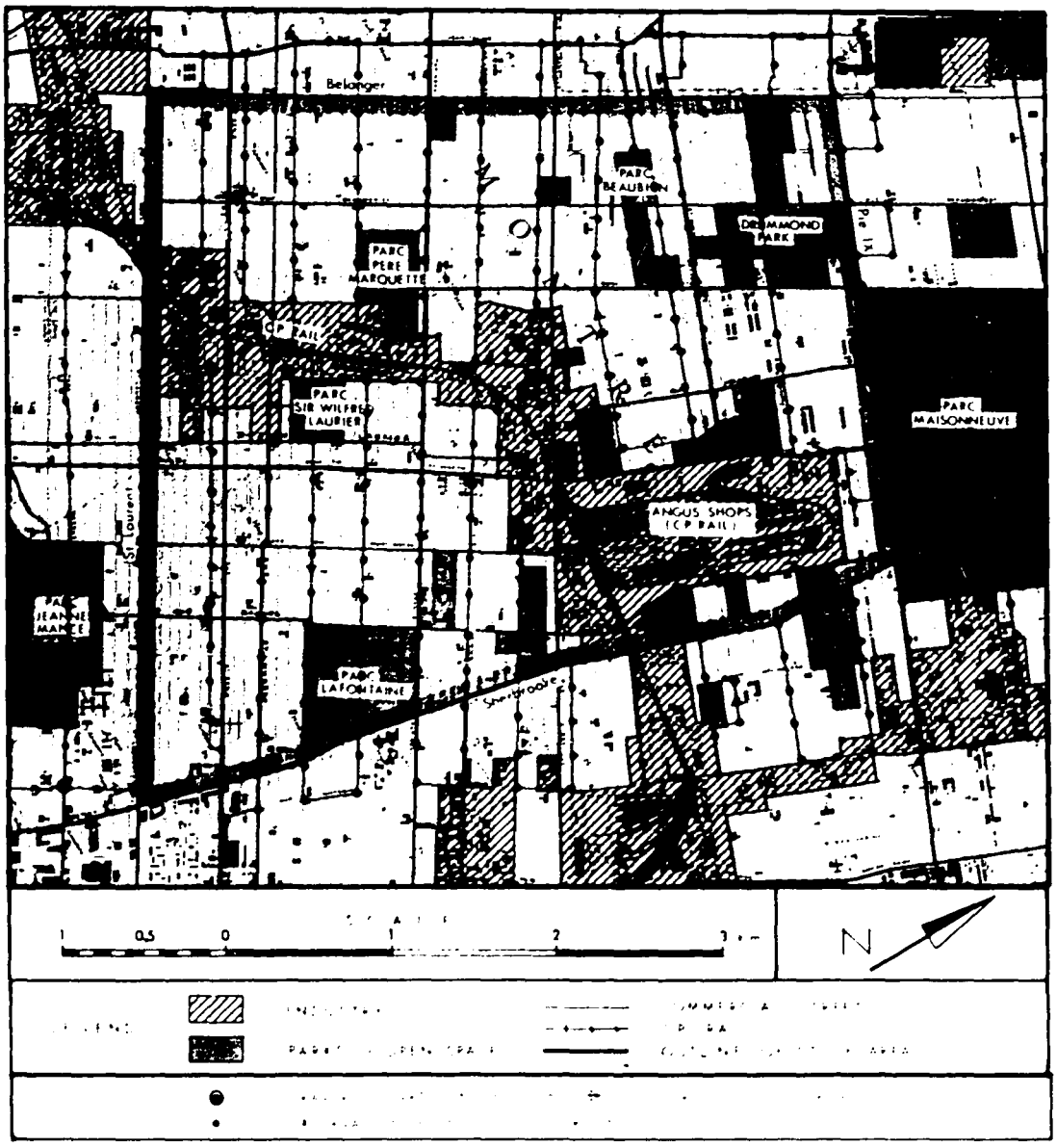
Belanger
PARC BEAUBIEN
DRUMMOND PARK
PARC PERE MARQUETTE
CP RAIL
PARC SIR WILFRED LAURIER
PARC MAISONNEUVE
ANGUS SHOPS (CP RAIL)
PARC LAFONTAINE
0,5
0
1
2
N

traffic it was possible to complete the route in 55 minutes; otherwise the traverse took the full hour.

The recorder was kept in continuous operation and check points were marked on the chart with the event marker. A log was kept of check points and times with a portable tape recorder. Initially, observations commenced in the early evening (2000 to 2200)[1] but it became apparent that it was necessary to start several hours before sunset; and the remainder of the traverses were started at least two hours before sunset, and continued every hour until just before sunrise. The dates and times during which observations were taken are shown in Table 2.

TABLE 2

Periods of Field Operation

Date	Times (EST)
November 27 - 28, 1969	2200 - 0400
December 16 - 17	2100 - 0600
17 - 18	2000 - 0600
February 7 - 8, 1970	1600 - 0700
14 - 15	1400 - 0600
March 30	1400 - 2200
31	1400 - 2300
May 14	1700 - 2100
July 23 - 24	1700 - 0500
24 - 25	1700 - 0500
27 - 28	1700 - 0500
29 - 30	1500 - 0500
August 4 - 5	1500 - 0500
5 - 6	1500 - 0500
6 - 7	1500 - 0500
7 - 8	1500 - 0500
8 - 9	1500 - 0500
9 - 10	1600 - 0500

1. Local Standard Time.

Wind and cloud information were obtained from St. Hubert Airport hourly aviation reports. Additional wind data were obtained from the Botanical Gardens meteorological tower and the CBC tower on Mount Royal.

b) Sampling Density

The area chosen for the analysis of sampling density was traversed by a route that extended beyond its boundaries so as to minimize boundary effects when plotting the isotherm maps. Continuous observations of air temperatures were taken along every third or fourth street that crossed the bands of commercial and industrial activity (Figure 8b), over a total area of 23.4 km^2. The route was 80 km long and required about three hours to complete, and was limited to a certain extent by the system of one-way streets in the area. Check points were marked on the chart with the event marker, and a log of points and times was kept with a portable tape recorder. Observations were usually commenced at least two hours after sunset, to allow air temperatures to stabilize. The dates and times during which observations were taken are shown in Table 3.

Linearity of change of ambient temperature was checked with the continuous record at the McGill Observatory. Wind data were obtained from McGill, the Botanical Gardens meteorological tower, and the CBC tower on Mount Royal.

TABLE 3

Periods of Field Operation

Date		Times (EST)
May	18 - 19, 1970	2330 - 0138
	28 - 29	2100 - 0020
	30 - 31	0000 - 0301
June	25 - 26	2230 - 0115
	28 - 29	2200 - 0047
July	26	2102 - 2355
	28 - 29	2115 - 0020
August	13	2309 - 0150
	14 - 15	2100 - 2354
	31	1900 - 2201

4. Weather Conditions

At the outset of this research, it had been hoped to confine observations of air temperature to nights on which there was no wind or cloud for the entire observation period. The impracticality of such a restriction rapidly became apparent and it was decided to broaden the limits acceptable for 'calm' and 'clear'. 'Calm' as used in this thesis includes winds up to 1.3 m sec^{-1}, and 'clear' includes up to 3/10 cloud if the cloud is cirrus, cirrostratus, altocumulus, but does not include even 1/10 of low or stratiform cloud (stratus, alto-stratus).

The restriction to calm and clear conditions was imposed in an attempt to simplify interpretation and analysis of the data. The complex interactions of the many factors that control air temperatures in an urban area are for the most part undefined; and this lack of knowledge makes it difficult to ascribe any particular change in air tem-

perature to any one, or combination of, these factors. It thus makes it difficult to explain or interpret the meaning of spatial or temporal variations in temperature patterns. To aid in investigating the effects of some of the remaining factors - such as urban fabric and structure - it was decided to hold wind and cloud cover 'constant' by imposing the restriction to calm and clear conditions. In addition, there is sufficient observational data in the literature to suspect that any definable relationships that do exist between factors and air temperatures would be most pronounced and therefore most easily recognizable under calm and clear conditions.

A difficulty with this type of approach is that there is no way of knowing beforehand whether the wind and cloud conditions on any given night will fulfill the required conditions. It is only after the fact, on checking the actual records of wind and cloud cover that one is able to determine how close the night had been to the specified conditions. As a result, the nights chosen for observations were found to have some hours when there was wind, cloud, or both in excess of the limits stated above. This had to be accepted and considered in the analysis.

A general description of weather conditions and other pertinent data for the nights of observation appears in Appendix I.

CHAPTER IV

SAMPLING DENSITY

This chapter analyses the general pattern of air temperatures in a large area of the City of Montreal based on a series of sampling densities comparable to those reported in the literature for similar studies of other cities, thereby allowing conclusions to be made regarding 'adequate' sampling densities for certain urban climate studies.

The density of observations required in a study of urban air temperatures will be determined by the specific objectives of the study. One which has as its objective the investigation of small scale features of the urban microclimate (the influence of a small park, one large building, a parking lot for example) requires a large number of observation points in the area immediately around the feature in question, giving a high density. On the other hand, a study whose objective is to analyse the general pattern of air temperatures within a whole city, or a district within the city, requires the points to be spread over a larger area, giving a lower density. It is possible that an extremely large number of observations may not be necessary to adequately depict the influence of the city on air temperatures.

1. Previous Studies

Estimates of sampling densities used in previous studies are given in Table 4. These computed densities have been rounded to the nearest

whole number. These data serve only as a means of comparison and do not imply that every square kilometer will contain the given number of points; indeed, it is quite possible that different densities were employed in various parts of the city. Ludwig (1967) points out that the spacing of his observation points was greater in the outlying areas than in the downtown area, but the actual number of points used was not reported. Ludwig states that this change in sampling density may account for the apparent lack of small scale temperature features in the outlying areas of the cities in his study. However the paucity of these small scale features may also be a result of the greater physical homogeneity in the residential districts.

The area referred to in Table 4 is the actual area surveyed, not necessarily the total incorporated area of the city. The population is included to provide a measure of city size.

There can be little doubt that a density of 20 or 30 points km^{-2} would provide considerable detail from which to analyse the pattern of urban air temperature variations. However, in using a density of this magnitude, one is working with a large number of observation points. In an area of 20 km^2 for example, a density of 20 or 30 points km^{-2} would necessitate observations at 400 to 600 points. In an analysis oriented towards an understanding of the general urban influence on climate, features consistent in fabric and structure over an area of several square blocks (10 square blocks for example) are the ones of major interest. There is a need to eliminate the influence of small scale spot sources of heat from the analysis. Observations at such a high density

TABLE 4

Sampling Densities From Selected Urban Studies

City	Population	Area (km^2)	No. of Points	Density (Pts km^{-2})	Author
Ogaki, Japan	75,000	4	120	30	Sekiguti (1964b)
Palo Alto, California	33,000	16	300-360	19-22	Duckworth and Sandberg (1954)
Corvallis, Oregon	21,000	17	130-150	8-9	Hutcheon et al (1967)
San Francisco, California	784,000	117	300-360	3	Duckworth and Sandberg (1954)
Hamilton, Ontario	300,000	111	200	2	Oke and Hannell (1970)
Uppsala, Sweden	30,000	46	79	2	Sundberg (1950)
Edmonton, Alberta	340,000	144	200	1	Daniels (1965)
Montreal, Quebec	2,500,000	350	364	1	Oke (1969)
Sheffield, England	534,000	86	99	1	Garnett and Bach (1966)
London, England	8,200,000	1550	78	1 pt/20 km^2	Chandler (1965)

are likely to include the influence of many small scale, essentially randomly distributed spot sources such as a bakery, a large air conditioner, a bus or truck idling by the side of the road, a roofer's tar furnace which would tend to complicate an attempt to evaluate the general urban influence.

One might also question the adequacy of a density of 1 point km^{-2} even though it has been frequently used. One observation point for each square kilometer of area seems a very small number of observation points to base a generalized analysis upon, since it only represents about one point in each 48 square blocks, to take an example from Montreal.

In view of the above, it was felt that a comparative study of the effectiveness of a series of densities between 20 points km^{-2} and 1 point km^{-2} would be productive in two ways. Firstly, in indicating an optimum density with a minimum number of observation points that would be satisfactory in depicting the general pattern of air temperatures in an urban area. Secondly, in providing a means of evaluating the adequacy of a low density such as 1 point km^{-2} in depicting general urban air temperature patterns.

2. Results for Montreal

As stated in Chapter III, the area chosen for the analysis of sampling density had to be a large area with uniform land use, little topographic variation, and easily accessible along a regular grid of streets. The most suitable area was found to be a 15.8 km^2 part of the dense residential area immediately north of Mount Royal bounded by St. Laurent, Sherbrooke, Pie IX and Belanger streets (Figure 8a). Observations were taken over a larger area of 23.4 km^2 in order to minimize boundary effects when plotting the isotherm maps. The size of the study area in relation to the island of Montreal can be seen in Figures 6 and 7.

This particular area is located approximately 5 km north of the main heat island core over the CBD of Montreal, and has been shown to be the location of a heat island cell (Oke and East 1971).

To carry out the comparative study, air temperatures at 200 m intervals along the traverse route were abstracted from the traverse charts, resulting in 339 observation points evenly distributed throughout the 23.4 km^2 survey area (Figure 8b). The temperatures at each observation point were reduced to a common time by applying a correction factor determined from the error of closure at several points along the traverse route.

Isotherm maps were constructed from a series of systematic samples taken from the population of observation points. The maps represent approximate sampling densities of 1 point km^{-2}, 4 points km^{-2}, 7 points km^{-2}, and 15 points km^{-2}. The following systematic samples were taken to give the required sampling densities:

every 14th point = 24 points = 1 point km^{-2}

every 4th point = 85 points = 4 points km^{-2}

every 2nd point = 170 points = 7 points km^{-2}

every point = 339 points = 15 points km^{-2}

The maps were drawn in order from low to high density, thus providing a less subjective interpolation in each case because there was no prior knowledge of smaller features evident with the higher density maps. Isotherms with 0.5 °C intervals were plotted, and the isotherm maps derived from the different sampling densities were compared to evaluate the relative effectiveness of each in depicting air tempera-

ture patterns. Results from only two nights of observations are presented as there was no significant variation in air temperature over the study area on the other eight nights of observations.

a) May 31, 1970

During the 3 hour period of observation, the wind was from the south between 2.7 and 4.0 m sec^{-1} and the sky was clear. The isotherm maps represent the air temperature pattern at approximately 0000 EST.

In plotting Figure 9 (1 point km^{-2}) the isotherms were placed largely by guesswork with this limited number of points. The resulting pattern is entirely different from that of the others for this date and as a result this density appears to be inadequate for the depiction of air temperatures in the study area.

Figure 10 (4 point km^{-2}) was the most difficult to draw as there were many areas where the placement of isotherms was indefinite. Certain features are clear, but in general the map differs considerably from both the inadequate 1 point km^{-2} and the subsequent maps at greater densities.

Figure 11 (7 points km^{-2}) was the easiest to draw, and there were only few areas where placement of isotherms was indefinite. The pattern shown is virtually identical to that for 15 points km^{-2}. All features are represented and the placement of isotherms coincides in general.

Figure 12 (15 point km^{-2}) was more difficult to draw. This density shows some small scale features causing excessive twisting and bending of isotherms. In many areas the placement of isotherms is indefinite. In general there was little change or improvement in pattern or placement of isotherms from the previous map.

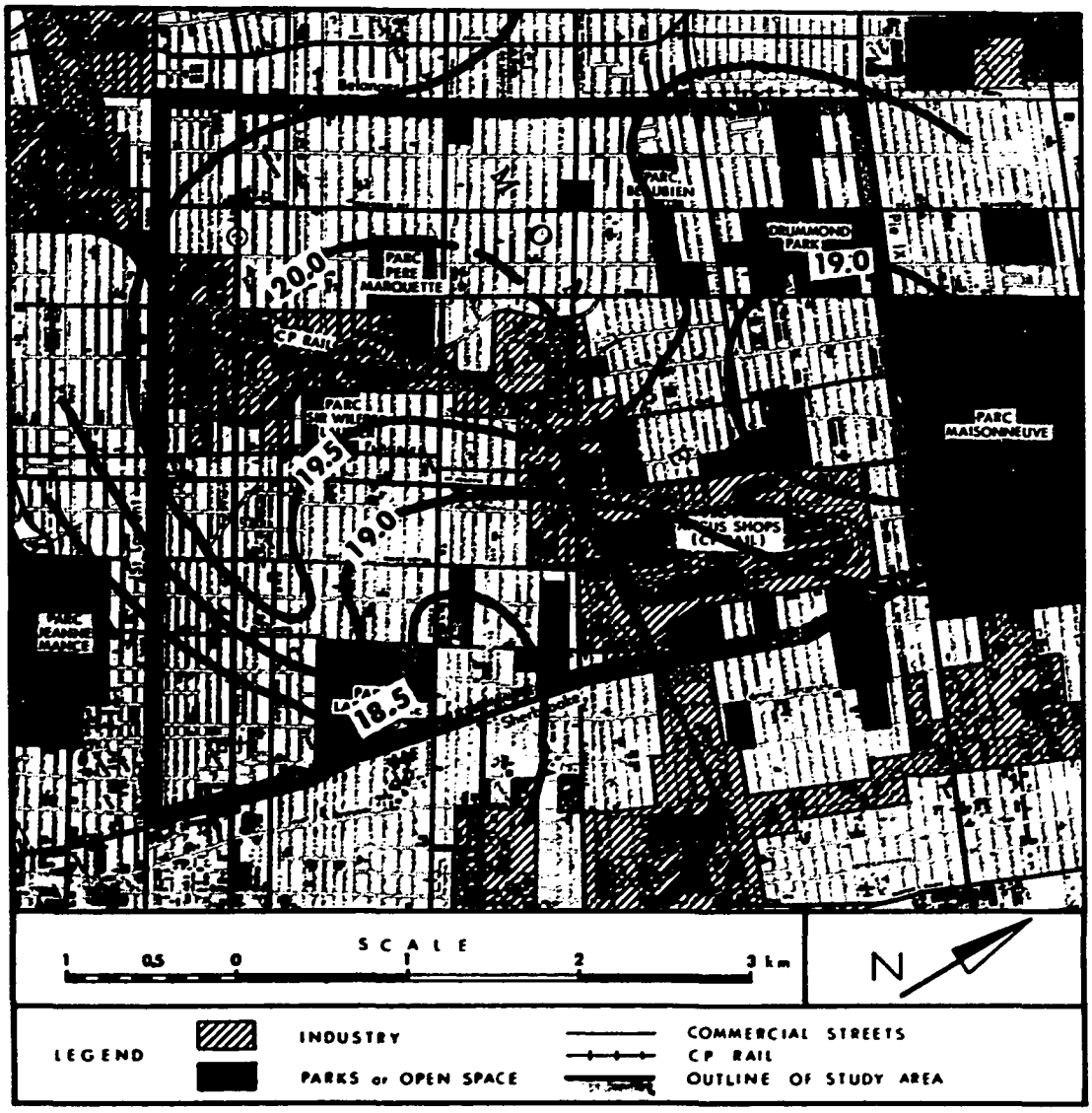

Figure 9: Air temperature pattern at 0000 EST May 31, 1970 based on a sampling density of 1 point km^{-2} (24 points).

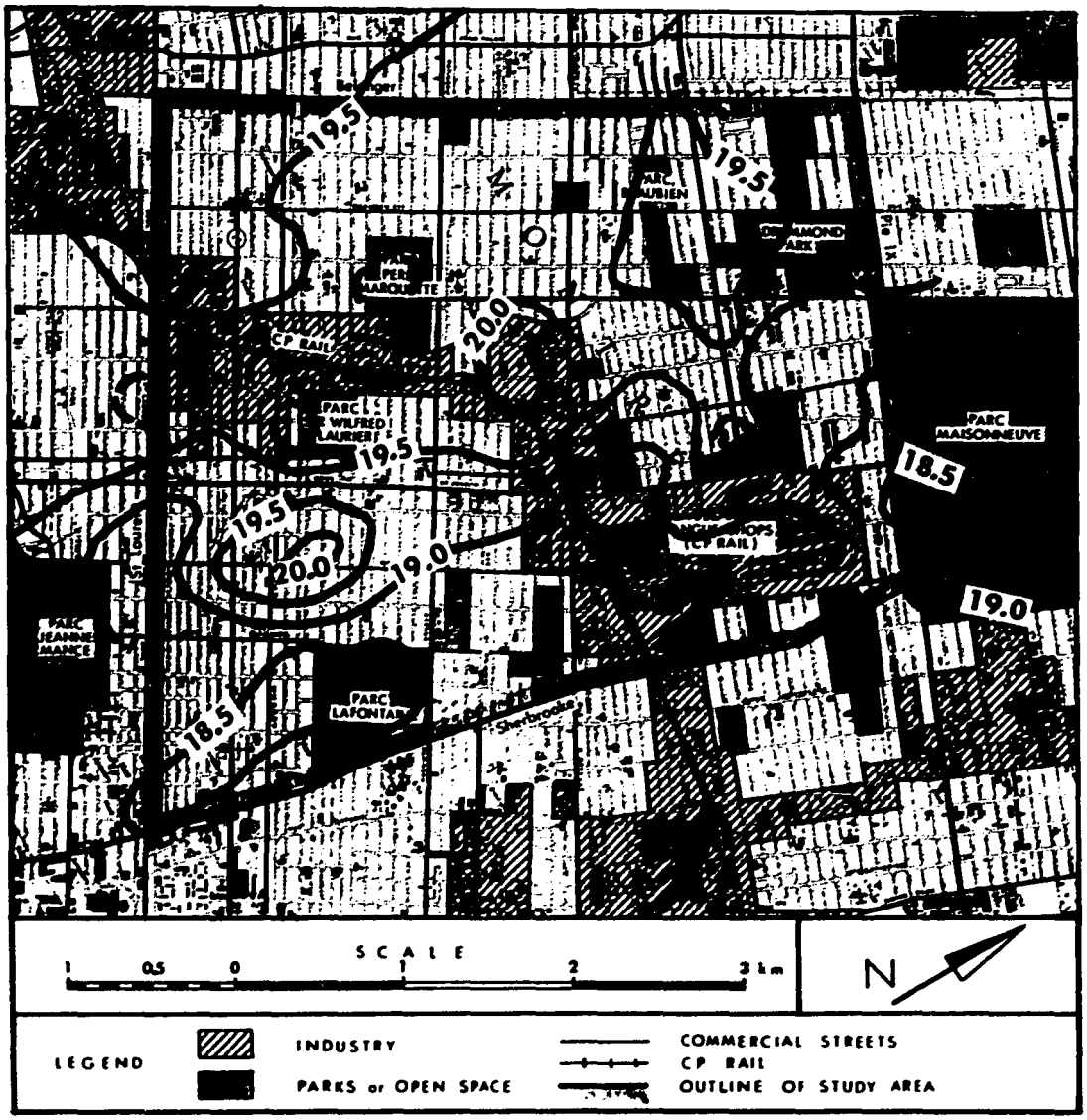

Figure 10: Air temperature pattern at 0000 EST May 31, 1970 based on a sampling density of 4 points km^{-2} (85 points).

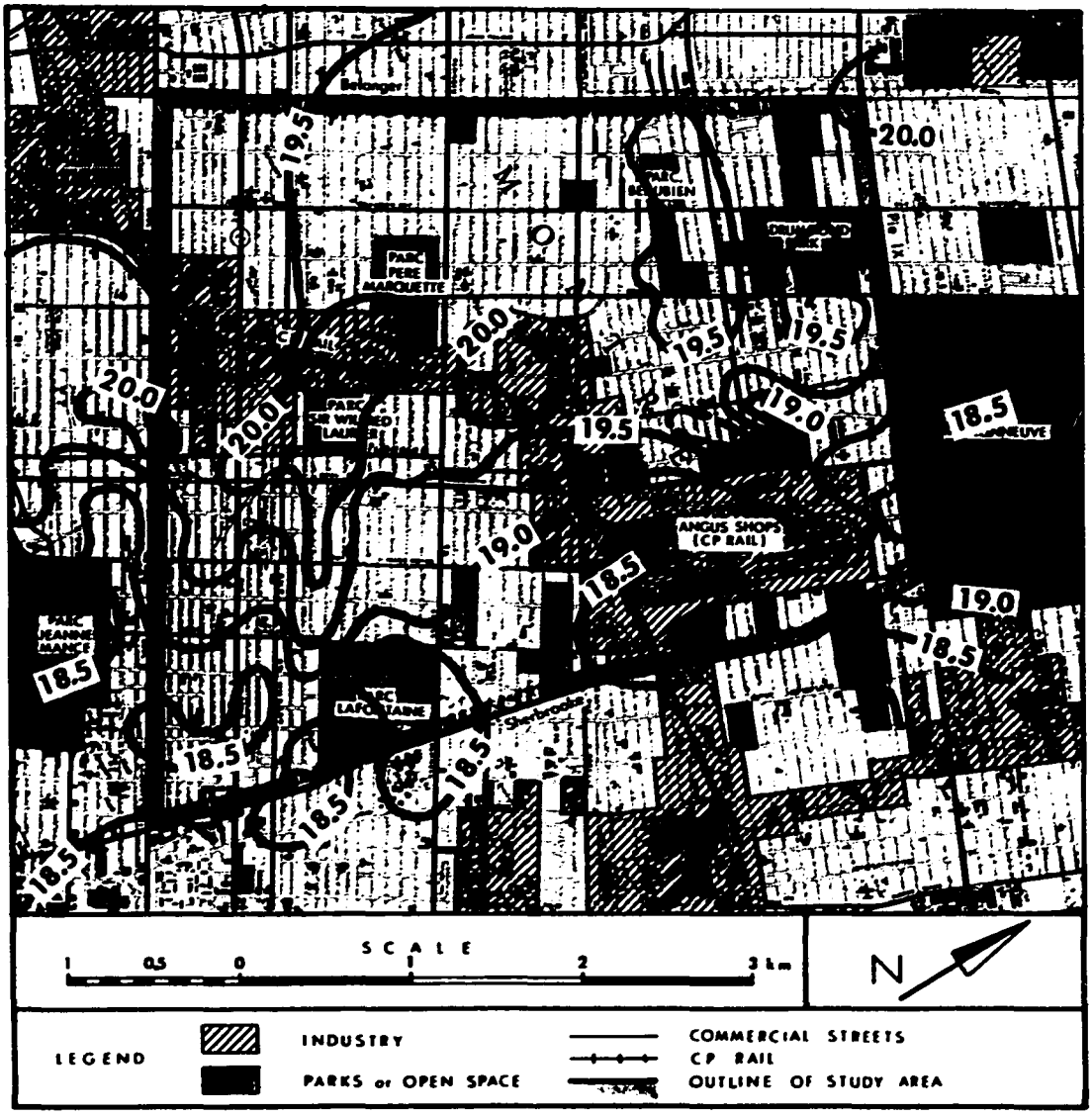

Figure 11: Air temperature pattern at 0000 EST May 31, 1970 based on a sampling density of 7 points km^{-2} (170 points).

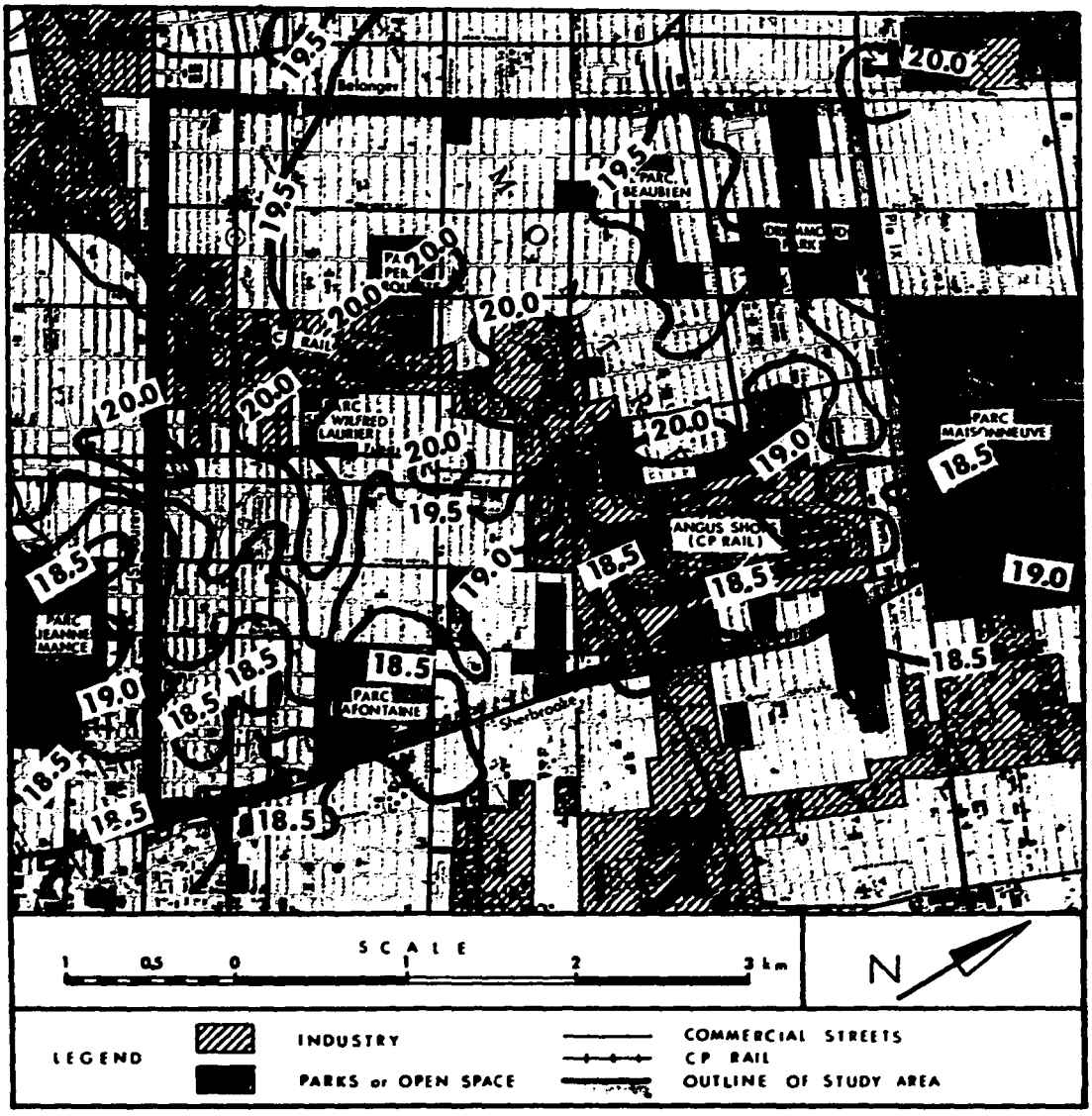

Figure 12: Air temperature pattern at 0000 EST May 31, 1970 based on a sampling density of 15 points km^{-2} (339 points).

b) August 31, 1970

During the 3 hour period of observation the wind was from the west between 4.5 and 6.7 m sec^{-1} and the sky was clear. The isotherm maps represent the air temperature pattern at approximately 1900 EST.

Figure 13 (1 point km^{-2}) omits many features evident in subsequent maps such as the three small cool spots in the northwest of the map, and the warm area along Pie IX. The outline of the large cool area around parc Pere Marquette is mainly guesswork, and the placement of the 15.5 ^{o}C and 16.0 ^{o}C isotherms differs from subsequent maps.

Figure 14 (4 points km^{-2}) shows the main features of the isotherm pattern and the placement of isotherms is very close to the placement on the two higher density maps. Interpretation of this map would be similar to that of the more detailed ones. This density made plotting relatively easy and only a few areas exist where the isotherms remain indefinite.

Figure 15 (7 points km^{-2}) clarifies the indefinite areas of the previous map and the extra observation points make it possible to locate the isotherms more precisely. The pattern shown here is virtually identical to that for 15 points km^{-2}.

Figure 16 (15 points km^{-2}) is the same as that for 7 points km^{-2} in pattern and placement of isotherms. At this density though, there are places where plotting strictly according to the rules leads to isotherms twisting and bending excessively, meaning that many small scale features are being shown. Such excessive fragmenting of the isotherms can tend to obscure the general pattern of air temperature and make interpretation more difficult. This tendency can be seen on this map, for example, by the breaking off of a small cell of 16.0 ^{o}C along St. Hubert Street.

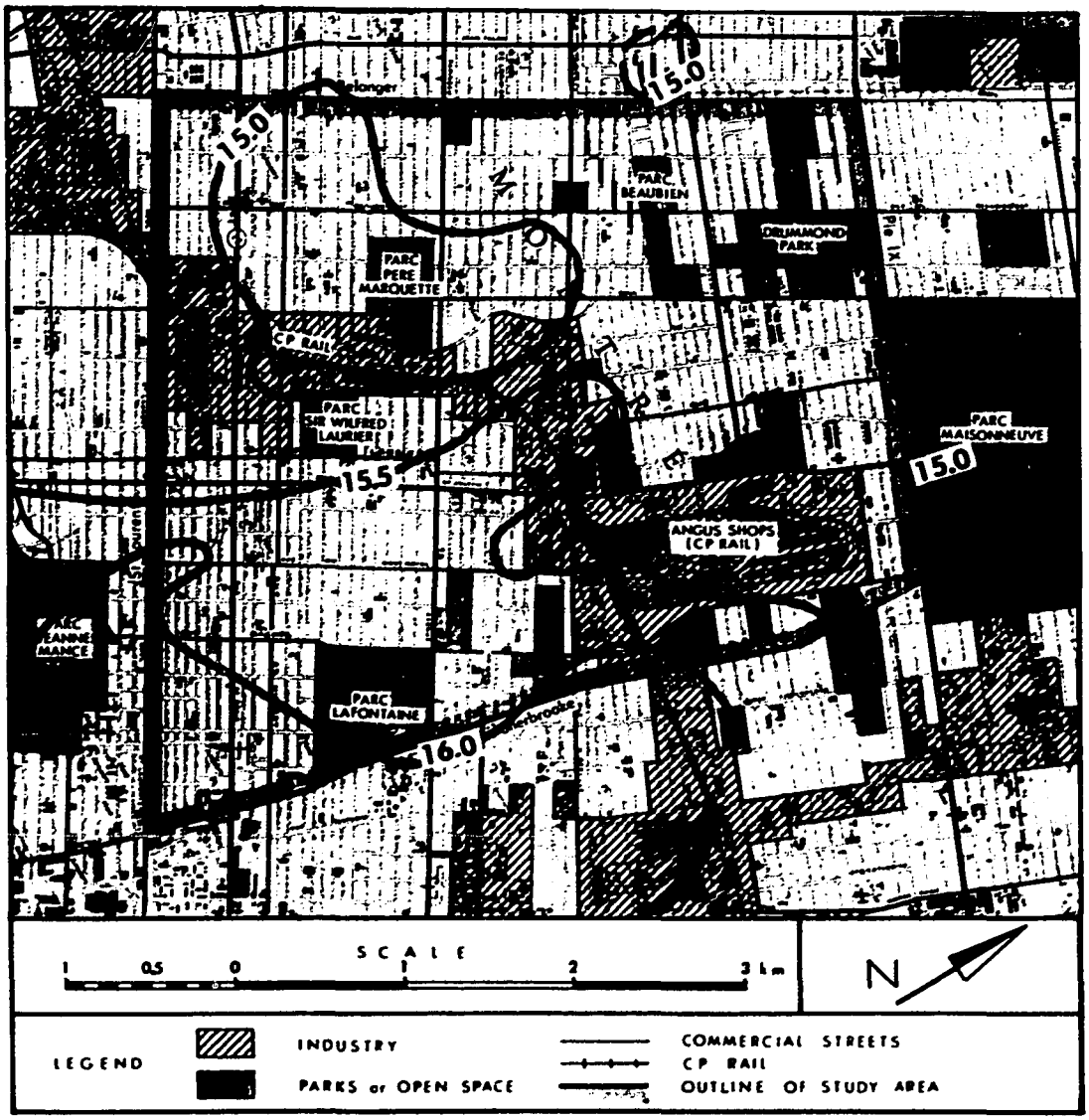

Figure 13: Air temperature pattern at 1900 EST August 31, 1970 based on a sampling density of 1 point km^{-2} (24 points).

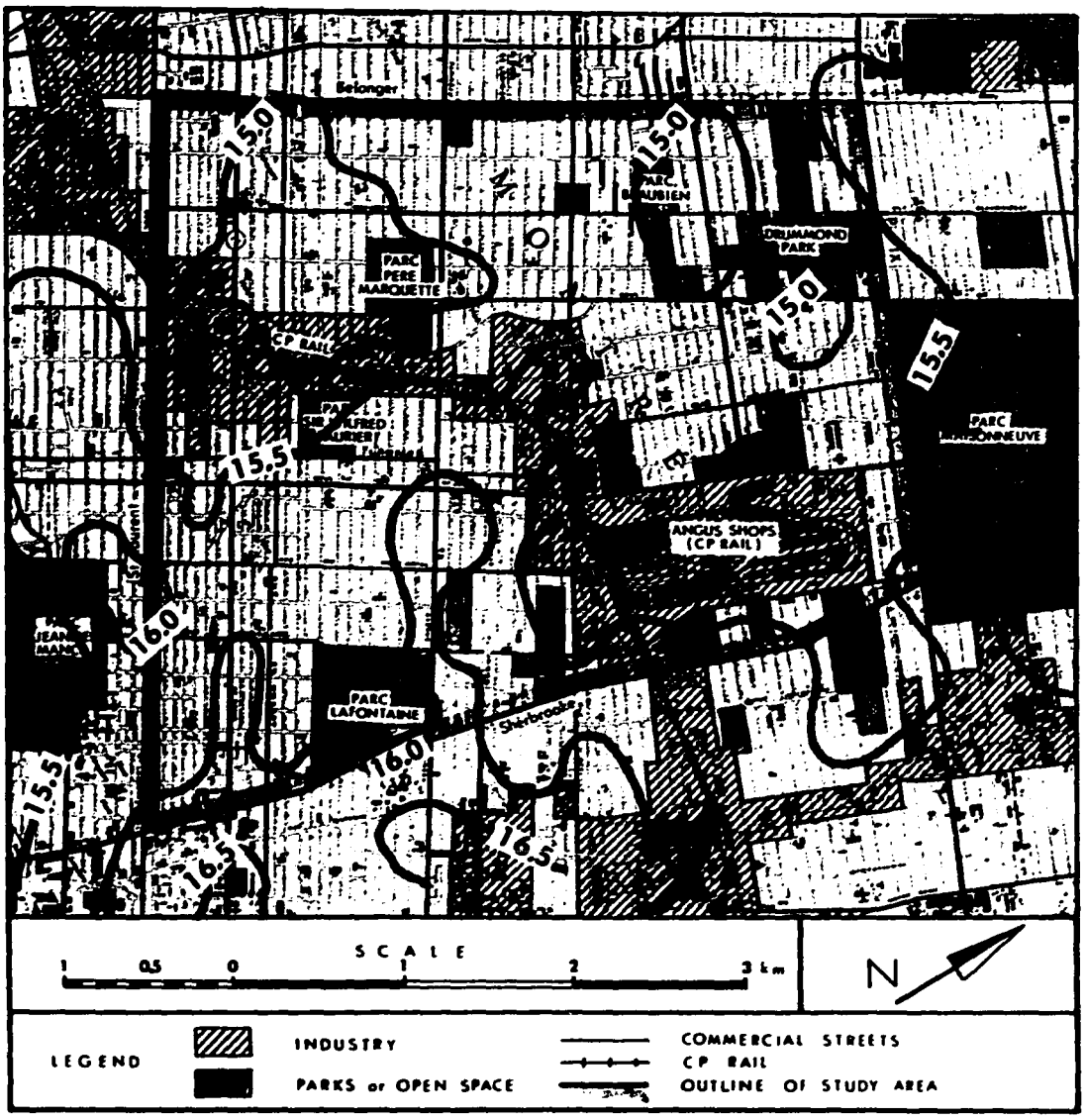

Figure 14: Air temperature pattern at 1900 EST August 31, 1970 based on a sampling density of 4 points km^{-2} (85 points).

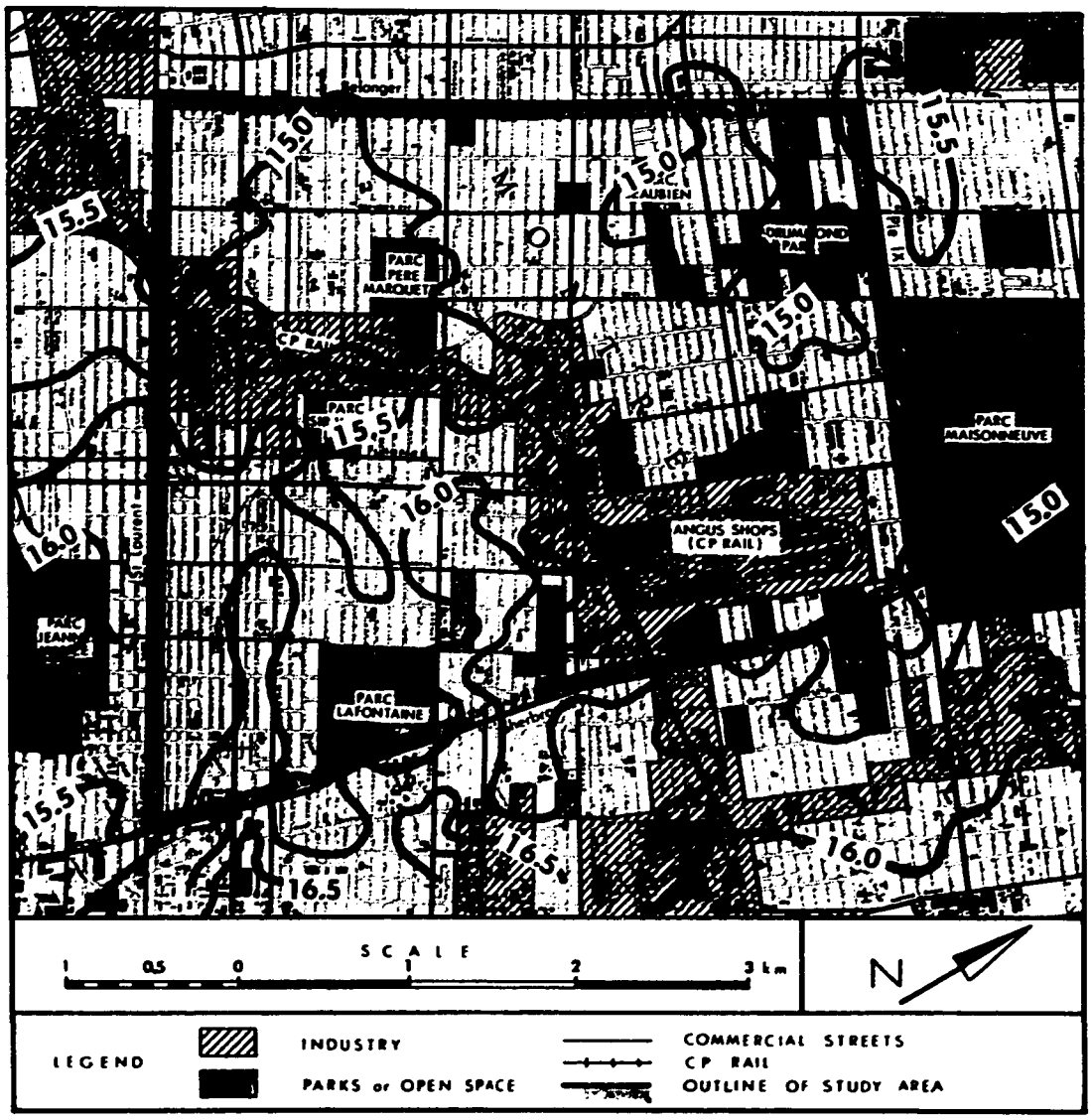

Figure 15: Air temperature pattern at 1900 EST August 31, 1970 based on a sampling density of 7 points km^{-2} (170 points).

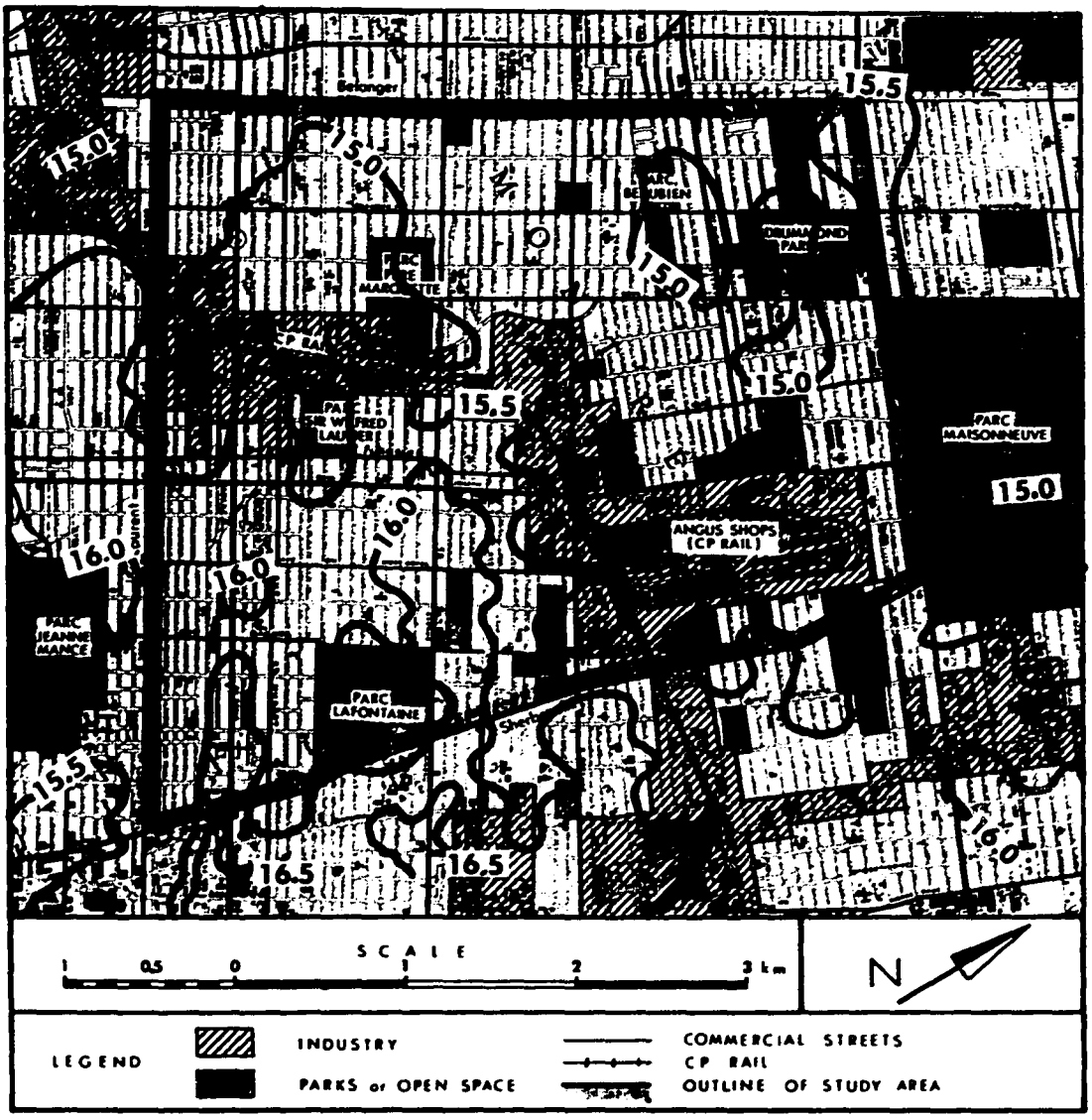

Figure 16: Air temperature pattern at 1900 EST August 31, 1970 based on a sampling density of 15 points km^{-2} (339 points).

c) Evaluation of Results

It would appear, firstly, that a sampling density of 1 point km^{-2} is not adequate to depict the spatial variations of air temperature in even the most generalized manner. This conclusion also implies that previous studies using low densities such as 1 to 3 points km^{-2} (Table 4) may be using seriously over-generalized isotherm maps in their analysis. The results presented in these studies may be missing important air temperature variations in the cities concerned, possibly the exact variations required to fulfill the objectives of the study.

Secondly, for a study with the objective of evaluating the general influence of the urban area on air temperatures, a density of 7 points km^{-2} appears to be the optimum. This density shows an adequate amount of detail in relation to the fabric and structure of the urban area, without requiring an excessive number of observation points. In fact 7 points km^{-2} gives virtually the same results as 15 points km^{-2}. However, it must still be remembered that a higher density would be required if the objective was to analyse the effects of microscale variations in fabric and structure as stated at the beginning of this chapter.

3. Interpretation of Air Temperature Patterns

The availability of isotherm maps for an urban area based on as great an observation density as those shown in Figures 11 and 15 prompts some detailed comment on the nature of the spatial patterns.

The 7 point km^{-2} isotherm map for May 31 (Figure 11) shows a distinct ridge through the centre of the study area formed by the 19.0 and 19.5 ^{o}C isotherms, with the northwest half of the area warmer than the southeast half. There appears to be a marked warm spot in the north corner of the area and several other warm cells near the edge of the industrial area. There seems to be cool air draining off the mountain (from the southwest) and flowing in a northeasterly direction along Sherbrooke Street with pockets below 18.5 ^{o}C flowing along with it. Cool spots are also evident in the west corner of the area, over parc Beaubien, and a third close to parc Beaubien. The temperature range on this map is from 18.1 to 20.3 ^{o}C and gradients of 0.5 $^{o}C \cdot 100\ m^{-1}$ occur in six places.

The 7 point km^{-2} isotherm map for August 31 (Figure 15) shows the northwest half of the map to be generally 0.5 ^{o}C cooler than the southeast half. The warmest area appears to be below Sherbrooke Street with tongues extending up St. Hubert and Papineau and warm spots near the intersection of St. Laurent and Mount Royal, and along Pie IX. Cool air appears to be flowing off the mountain through Jeanne Mance Park and distinct cool spots occur near parc Pere Marquette, parc Beaubien, Drummond Park, and along Sherbrooke Street in parc Maisonneuve. The 15.5 ^{o}C isotherm outlines the boundary of the industrial area, and parc Lafontaine appears to be 0.5 ^{o}C cooler than its surroundings. The temperature range on the map is from 14.5 ^{o}C to 16.7 ^{o}C and gradients of 0.5 ^{o}C 100 m^{-1} occur in three places.

Certain points are notable on the two maps. Firstly, the temperature range within the study area is 2.2 °C in both cases, indicating that temperature variations related to distinct land-uses within a small area of the city of Montreal are possible under favourable meteorological conditions. However, such a variation within a city casts some doubt on the validity of the heat island intensity value of 2.5 °C assumed by Delage and Taylor (1970) in their heat island circulation model. Secondly, cool air drainage off Mount Royal appears to have an important influence in the particular area studied. Thirdly, parks and open spaces are characterized by temperatures approximately 0.5 °C cooler than the surroundings. These two observations have important implications for urban planners and architects who are concerned with the effects their planning and buildings might have on the urban climate. In general, cool air drainage such as this should be utilized to improve air circulation within the immediate area by the proper design and location of buildings and streets. The cooling effect of parks and open spaces is already well known, but should be re-emphasized to those planners and architects who wish to create concrete deserts around their developments.

Fourthly, there appears to be a distinct division of the study area into two temperature regimes with a noticable temperature 'cliff' dividing them. This division is related to the division of the study area in two parts by the band of industry along the C.P. Rail tracks. This break in the uniformity of structure and fabric within the area provides a natural boundary for a change in air temperature regimes, by itself or in combination with an external influence such as the cool air drainage from Mount Royal. An air flow such as this is likely to be channelled by

a variation in the form and structure of the urban surface. Fifthly, main traffic arteries appear to give rise to distinct warm spots or tongues, as would be expected from the localized energy input in the form of the exhaust from motor vehicles and the concentration of human activity along such arteries.

Sixthly, the maximum temperature gradients observed in Figures 11 and 15 are equivalent to a gradient of 5.0 $^{o}C\ km^{-1}$, and as such are greater than gradients that have been observed at the edge of the heat island. Daniels (1965) has shown typical nocturnal gradients in Edmonton to be around 4.0 $^{o}C\ km^{-1}$ under favourable conditions, and Oke and Hannell (1970) have observed a maximum gradient at the boundary of the heat island in Hamilton, Ontario of 3.8 $^{o}C\ km^{-1}$ under ideal conditions. Oke and East (1971) report that extreme gradients of 4.0 $^{o}C\ km^{-1}$ have been observed at the boundary in Montreal. Since the thermal gradient at the edge of the heat island is known to generate thermal breezes (Chandler 1961) the gradients observed in Montreal are likely to generate thermal winds within the city itself. Such winds may be important in the dispersion of air pollutants, and the amelioration of block size microclimate by improving air circulation. In addition, this observed gradient corroborates the choice by Delage and Taylor (1970) of a thermal gradient of 5.0 $^{o}C\ km^{-1}$ as one of the assumptions inherent in their heat island circulation models.

In general, the pattern of air temperature seems to be a multi-cellular one as opposed to a gradual smooth variation over the area studied. This multi-cellular type of pattern has been hinted at previously in Montreal (Oke and East 1971) but the sampling density in that study was not adequate to indicate the character of the pattern. This

multi-cellular pattern may be important in producing local circulation cells which could have important implications in air pollution dispersion (Yap, Gunn and East 1969). Such local complications will develop considerable problems for future attempts at urban dispersion modelling, especially on the local rather than city-wide scale as referred to by Gold (1956).

CHAPTER V

HEAT ISLAND INTENSITY

This chapter examines in detail the nocturnal development of ΔT_{u-r} and relates the heat island growth and decay dynamics to the variations in and differences between observed urban and rural cooling rates.

Heat island intensity was computed as the difference between the highest urban (CBD) and lowest rural air temperatures observed for each hour during each observation night. Times were normalized with respect to sunset. The hour during which sunset occurred was designated as hour zero, and previous and subsequent hours numbered as negative and positive hours respectively. This conversion was necessary to facilitate computation of seasonal and composite means.

1. Nocturnal Variation of ΔT_{u-r}

In order to arrive at general values for ΔT_{u-r} in winter and summer, mean values were computed for each hour of the late afternoon and night from all nights of observations during the summer and winter. The mean values obtained were then combined to arrive at composite figures for the two seasons. This procedure was followed without regard for wind or cloud conditions as it was desired to obtain a broad sample. Mean and standard deviation of wind speeds ($\bar{u}$ and σ_u) and cloud amounts ($\bar{c}$ and σ_c) were computed for the 11 summer nights and seven winter nights of observations (Table 5).

TABLE 5

Mean Wind Speed and Cloud Cover Characteristics on Observation Nights

Season	$\bar{u}$ m sec^{-1}	σu m sec^{-1}	$\bar{c}$ tenths	σu tenths
Summer	1.6	±1.6	0.2	±0.3
Winter	1.5	±1.4	0.2	±0.2
Combined	1.6	±1.5	0.2	±0.2

It can be seen that the nights of observations were characterized by light winds and scattered cloud.

Figure 17a shows values of ΔT_{u-r} computed from the 11 nights of summer observations. The smoothness of the transition from the afternoon values of around 3.0°C to the nocturnal values of between 7.0 and 9.0 °C, and the consistency of ΔT_{u-r} between sunset and sunrise are notable. A consistent energy input to the urban air during the transition period around sunset could give rise to such a steady build-up of the heat island, and the most likely source for such energy in the summer is the energy stored in the urban fabric (G). In contrast to the summer, mean values in the winter (Figure 17b) show a greater variability. Afternoon values are consistent between 3.0 and 4.0 °C but the build-up of ΔT_{u-r} is not as well defined, and intensities range from 4.0 to 7.0 °C. It is possible that this greater variability is related to the smaller sample (seven nights) in winter, but could also reflect the variability of

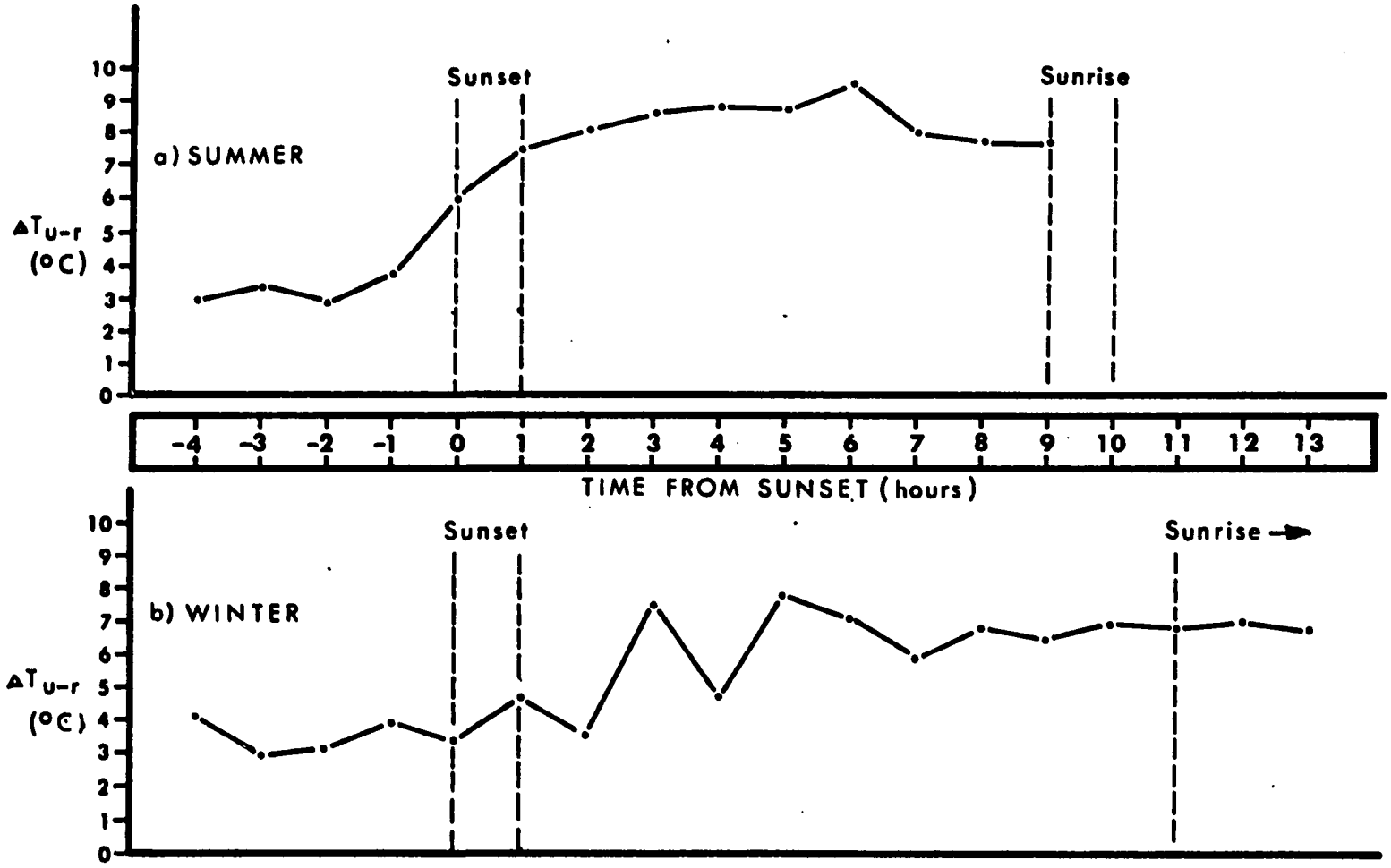

Figure 17: Mean values of ΔT_{u-r} computed from, a) 11 nights of summer observations and, b) 7 nights of winter observations with light winds and scattered cloud.

artificial heat generation which is a major source of energy on winter nights.

The combination of the above seasonal means is shown in Figure 18. This composite curve emphasizes the general nature of ΔT_{u-r} variations over the night. The general pattern appears to be one of quick growth around sunset, slower growth until the peak is reached then the slight drop in value and stabilization for the remainder of the night.

Figure 19 shows histograms of hourly ΔT_{u-r} values for winter, summer and the combination of the two. It can be seen from the diagrams for winter and summer that the most common intensities tend to be about 1 ^{o}C higher in summer. The peaking of frequencies is more pronounced in summer due to the larger sample but the percentage of observations in the most common class is almost the same (20% in the winter, 22% in the summer). There is also a secondary peak evident in both winter and summer diagrams in lower intensities around 2.0 to 3.9 ^{o}C (15% in winter and 11% in summer). These values occur mainly in the late afternoon.

From these histograms and the average values shown in Figures 17 and 18 it is possible to specify typical nocturnal ΔT_{u-r} values in Montreal, under light winds and scattered clouds. The most notable common features to both seasons are, firstly, the consistent low (around 3.0 ^{o}C) late afternoon values and secondly, the stabilization around 8.0 ^{o}C in the summer and around 7.0 ^{o}C in the winter following the maximum ΔT_{u-r} for the night. Intensities on summer nights tend to be greater than those observed in winter, and considering all winter and summer nights together, the most common ΔT_{u-r} values are between 8.0 and 8.9 ^{o}C.

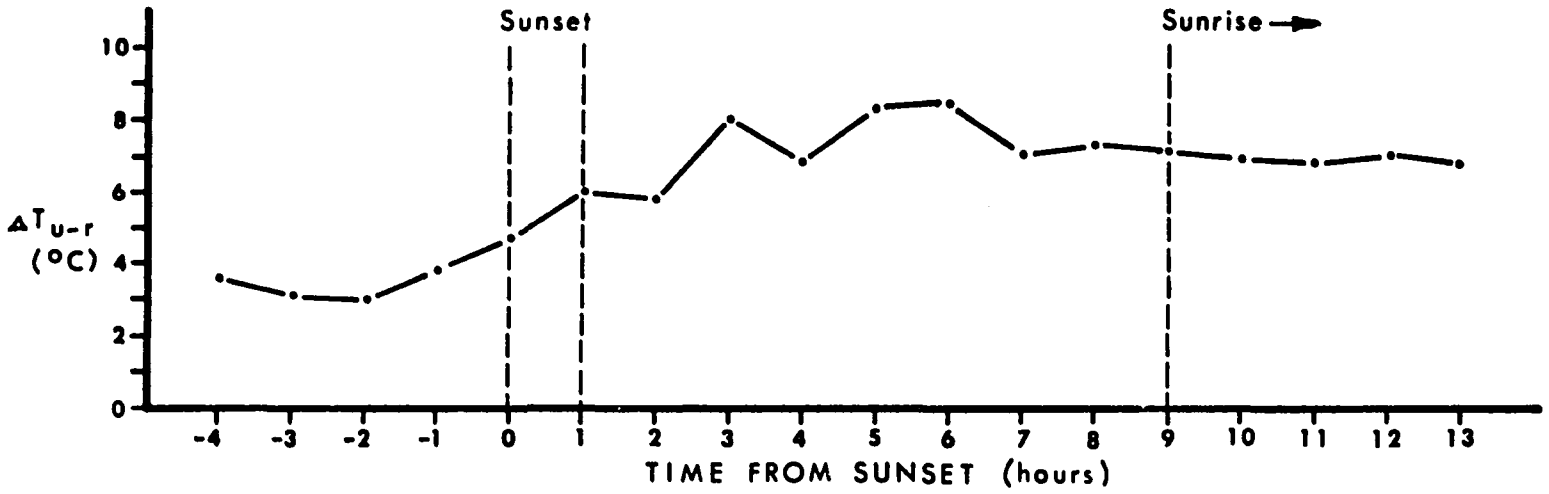

Figure 18: Mean values of ΔT_{u-r} computed from 18 nights of observations (summer and winter combined) with light winds and scattered cloud.

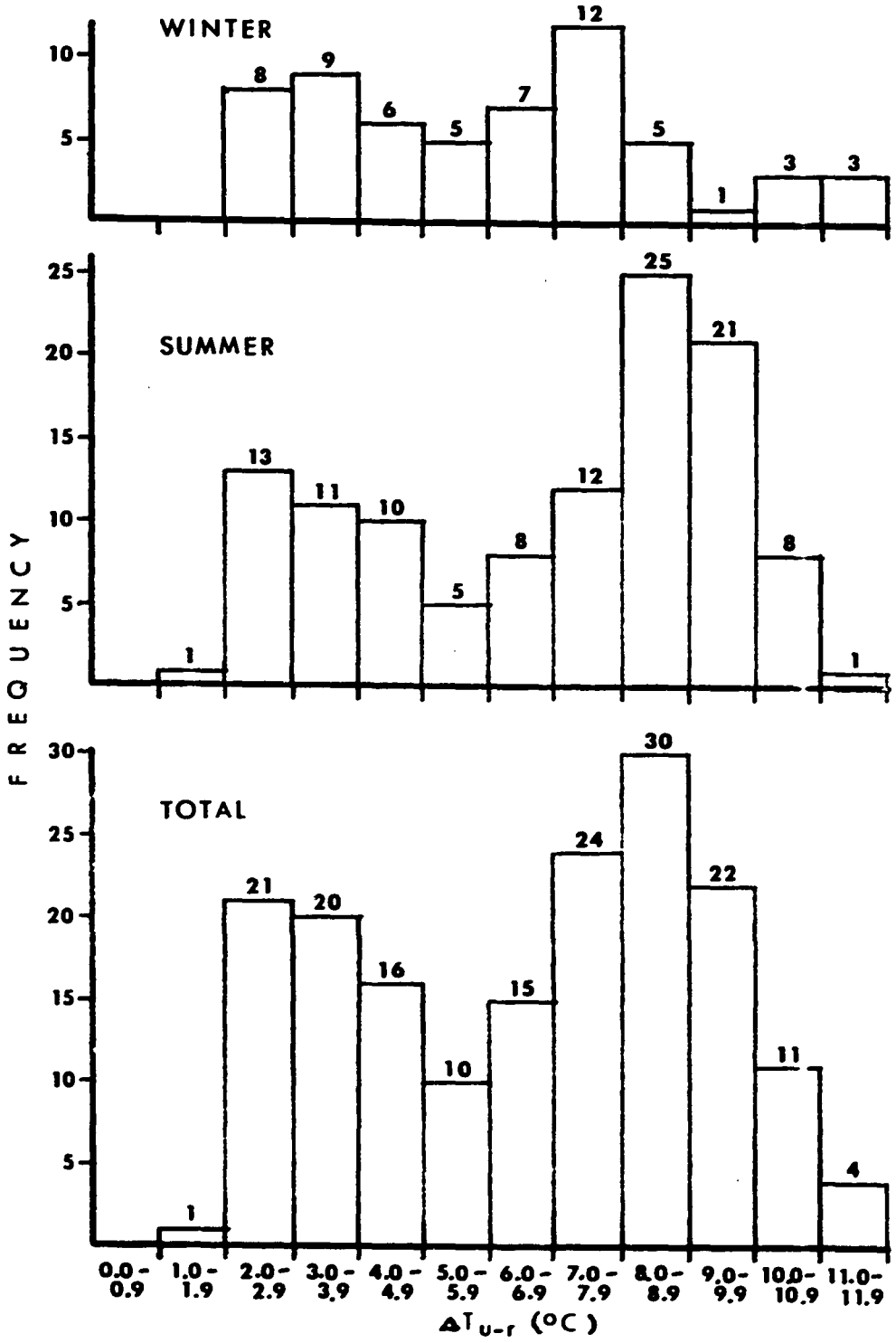

Figure 19: Histograms of hourly ΔT_{u-r} values.

2. Urban/Rural Cooling Rates

In order to more fully understand the mechanism by which ΔT_{u-r} grows and decays, the actual cooling rates ($\Delta T/\Delta t$) for the CBD and the rural area are compared.

An indication of the diurnal variation of $\Delta T/\Delta t$ values to be expected in downtown Montreal is available from a thesis by Godin (1969), but a similar analysis for a rural station is not available. Godin analysed $\Delta T/\Delta t$ from a study of continuous records of air temperatures on the McGill University campus 0.5 km NW of the main core of the CBD. These rates were derived from diurnal temperature traces that are averages of 20 sunny days in each month of the year. Figure 20 shows the diurnal variation in $\Delta T/\Delta t$ ($^{o}C\ hr^{-1}$) with months of similar diurnal variation grouped together as presented by Godin.

The change from warming to cooling rates appears to occur at around 1500 for the months of July through January. This would be 2.5 to 4.5 hours before sunset during the months of July, August and September, and 1 to 2 hours before sunset during the months of December and January. The change occurs slightly later, about 1530, during the months of February and March, which would be 1.5 to 3 hours before sunset.

The maximum cooling reported by Godin is approximately -1.0 $^{o}C\ hr^{-1}$. This occurred shortly after sunset during the months of April through September. During the night, $\Delta T/\Delta t$ tends to decrease gradually attaining a value of approximately -0.5 $^{o}C\ hr^{-1}$ shortly before sunrise. A change to warming from cooling occurs around sunrise. The remaining months (October through March) appear to attain a cooling rate of -0.4

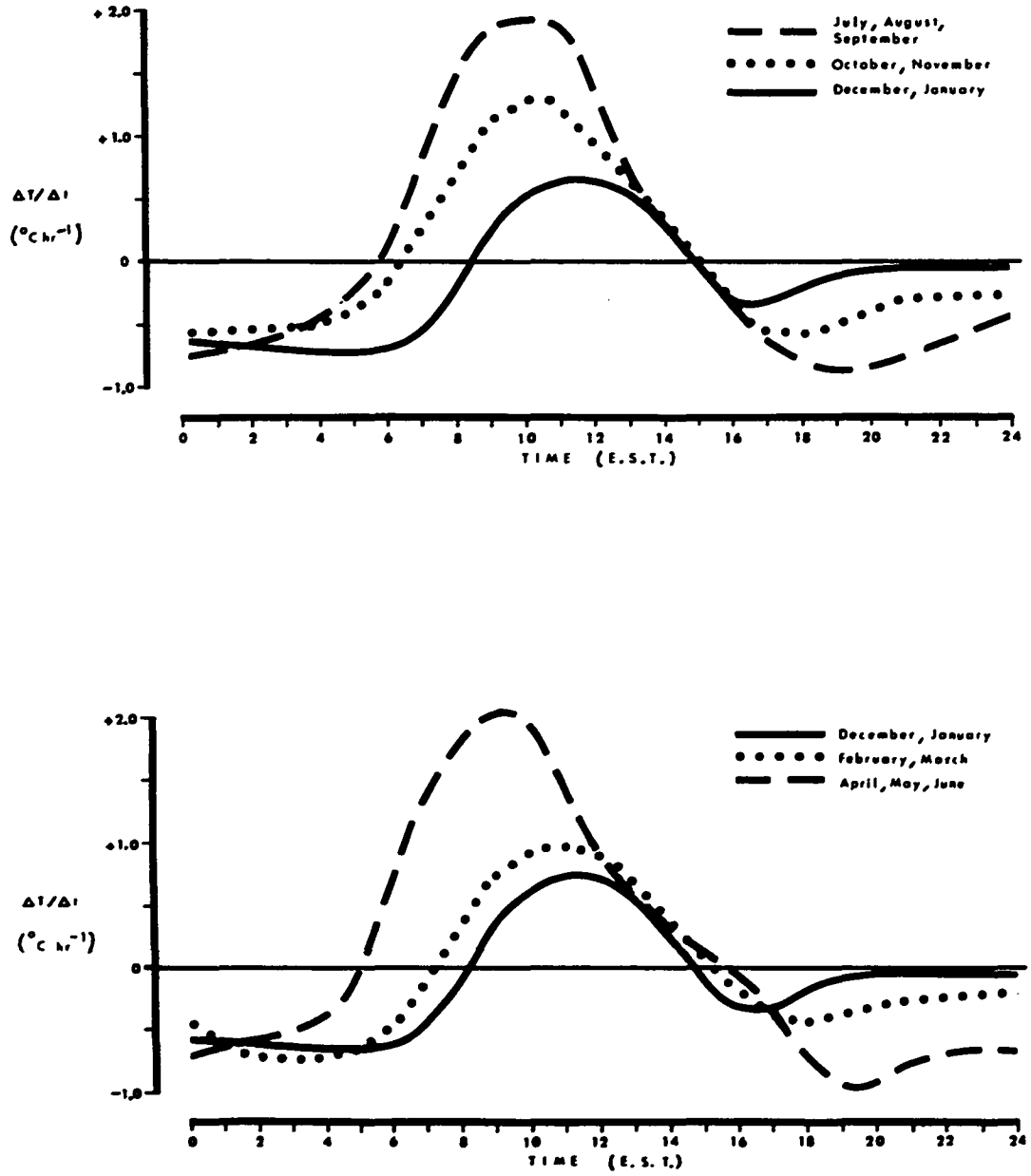

Figure 20: Diurnal variation in $\Delta T/\Delta t$ with months of similar diurnal variation grouped together (after Godin 1969).

$^{o}C\ hr^{-1}$ around sunset, but the variation in $\Delta T/\Delta t$ over the remainder of the night is unclear.

In the present study cooling rates were calculated from hourly temperature observations in the CBD in Montreal and a rural area nearby (Figure 7). Temperature observations at a series of points within each area were averaged to arrive at a spatial average within each area. This 'area' temperature was then compared with the 'area' temperature one hour before, the difference giving the warming or cooling. Since time periods of one hour were used this measured difference gives the rate of change directly ($^{o}C\ hr^{-1}$). Hourly cooling rates were calculated for all nights of observations in this manner, resulting in a time series of cooling rates for each night. These individual time series were then grouped into summer and winter sets of observations, and mean values of $\Delta T/\Delta t$ for each hour of the late afternoon and night were computed for each set of observations (11 summer nights and seven winter nights). Times were normalized with respect to sunset in the same manner as in the previous section.

a) Cooling Rates - Summer

The CBD cooling rates in Figure 21 a and b are in good agreement with those reported by Godin. The greatest cooling appears to occur following sunset and then $\Delta T/\Delta t$ tends towards a low constant value of around $-0.7\ ^{o}C\ hr^{-1}$ for the remainder of the night. Figure 21b shows cooling rates for a sub-set of summer nights that were completely calm and clear for at least 8 hours following sunset, and it can be seen that there is virtually no difference in the CBD $\Delta T/\Delta t$ from Figure 21a where

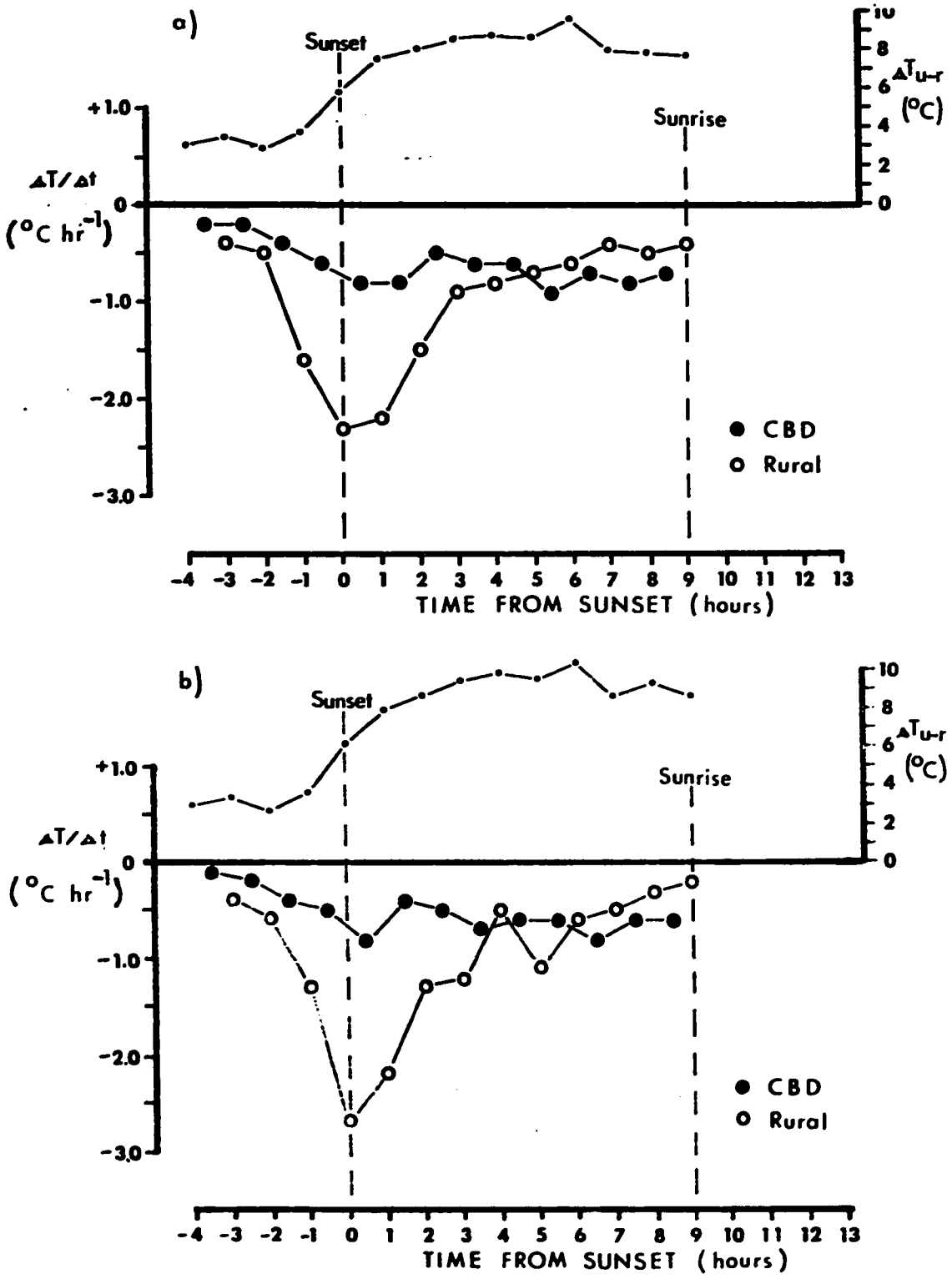

Figure 21: Mean hourly $\Delta T/\Delta t$ and ΔT_{u-r} in summer computed from a) 11 nights with light winds and scattered cloud and b) 4 calm and clear nights.

there was some influence from wind and cloud (Table 5). It would thus appear that winds and cloud cover had little effect on cooling rates in downtown Montreal on the summer nights considered here.

Rural cooling rates, on the other hand do appear to be more sensitive to variations in wind and cloud. The main differences evident under the calm and clear conditions in Figure 21b are that the maximum rural cooling is 0.4 $^{o}C\ hr^{-1}$ greater (at -2.7 $^{o}C\ hr^{-1}$) and $\Delta T/\Delta t$ tends to be more variable. The rural cooling rate attains its maximum value at sunset, as would be expected considering the general diurnal variation of air temperatures. This is one hour earlier than the urban maximum, and the two rates tend to equalize at about 5 hours after sunset. Urban and rural $\Delta T/\Delta t$ then maintain approximately the same value for the remainder of the night, and the urban area cooling at a slightly stronger rate.

A comparison of the CBD and rural cooling rates enables one to trace the growth of ΔT_{u-r} throughout the night (Figure 21a and b). The cooling rate in the rural area is slightly greater in the late afternoon then increases sharply 2 hours before sunset, and ΔT_{u-r} starts to build about one hour after the rural cooling rate starts to increase. The heat island is formed for the most part while the rural $\Delta T/\Delta t$ is at its maximum value around sunset, although ΔT_{u-r} does not attain its maximum value until several hours later. The time of occurrence of maximum ΔT_{u-r} is discussed at the end of this chapter. ΔT_{u-r} ceases building as fast about one hour after rural $\Delta T/\Delta t$ attains its maximum value, as the rural $\Delta T/\Delta t$ decreases as sharply as it had increased. Maximum ΔT_{u-r} is reached about one hour after the two cooling rates equalize, then

ΔT_{u-r} decreases slightly to what appears to be its equilibrium value around 8.0 °C as the CBD is now cooling at a slightly greater rate than the rural area. ΔT_{u-r} remains at this value for the rest of the night because both the CBD and rural areas are cooling at approximately the same constant rate. The calm and clear conditions of Figure 21b result in an absolute value of ΔT_{u-r} one to two degrees greater in the hours following sunset, as a result of the greater maximum rural $\Delta T/\Delta t$.

b) Cooling Rates - Winter

The observed CBD cooling rates for the general winter case (Figure 22a) clarify the uncertainty of the results obtained by Godin. The change from warming to cooling takes place about two hours before sunset, and $\Delta T/\Delta t$ attains a value of around -0.3 °C hr^{-1} at sunset then oscillates around this value for the remainder of the night. On the calm and clear nights (Figure 22b) the CBD maintains a constant temperature ($\Delta T/\Delta t = 0$) for the five hours following sunset, and then the maximum cooling occurs.

One explanation for this abnormal variation could be that sunset in the winter (December through February) occurs just prior to the evening rush hour. Energy released into the urban air from motor vehicles during the rush hour, and increased space heating energy releases as air temperatures begin dropping are sufficient to maintain urban air temperatures at their sunset values for several hours. With no wind, any energy released into the urban air (and the urban fabric will also release energy) will tend to remain concentrated near its source and oppose urban cooling

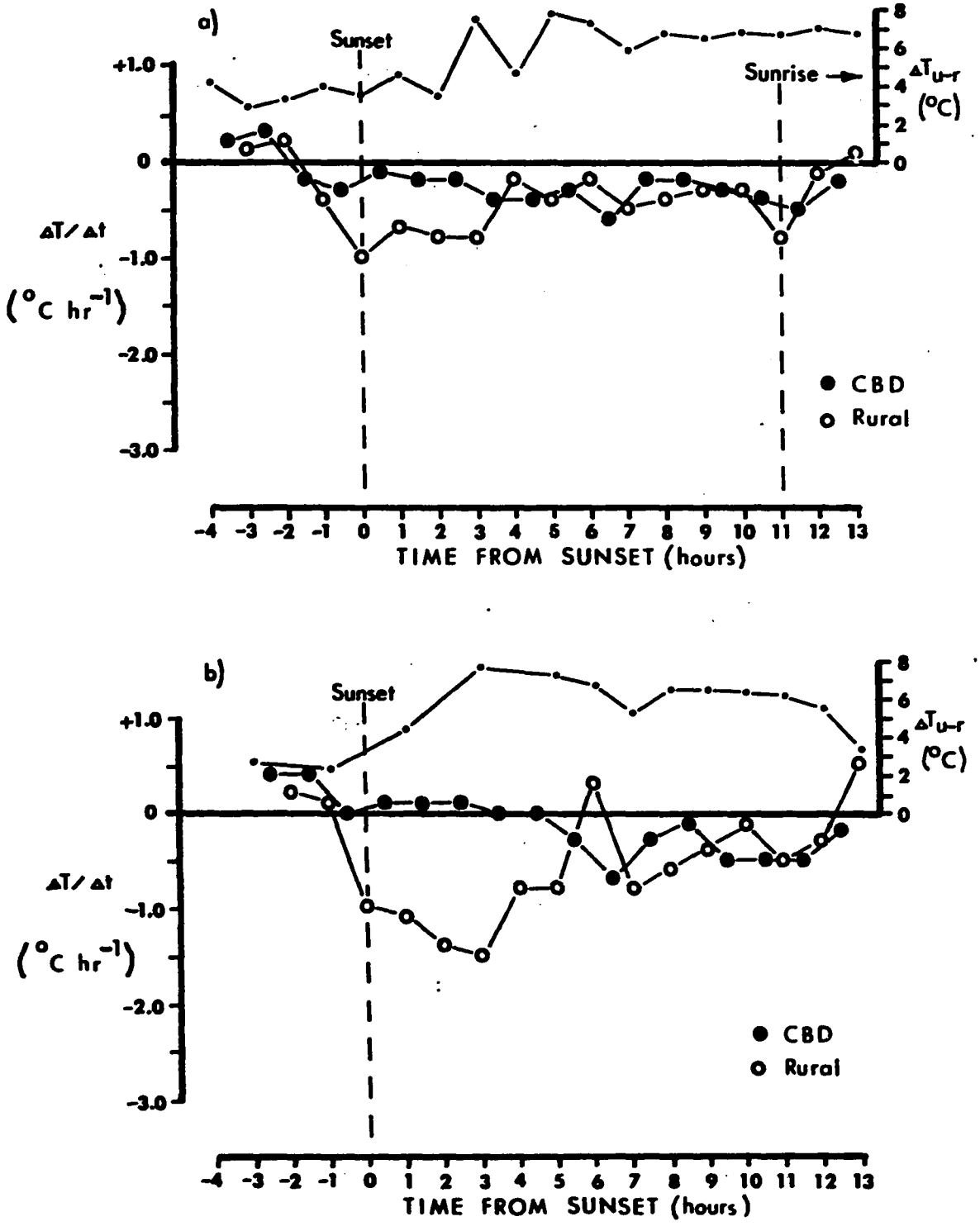

Figure 22: Mean hourly $\Delta T/\Delta t$ and ΔT_{u-r} in winter computed from,
a) 7 nights with light winds and scattered cloud and,
b) 3 calm and clear nights.

at that location. Since energy released from motor vehicles and space heating originates from many individual sources distributed evenly over the urban area, the net result is that cooling of the air in the CBD is delayed for several hours.

Bach (1970) estimates that 2/3 of the artificial heat generation (F) originates from stationary sources (industrial, domestic and commercial combustion) and 1/3 from mobile sources (motor vehicles), over a 24 hour summer day in Cincinnati. It is not known if the same proportion applies in winter in Montreal, but these figures give some idea of the relative importance of the two types of sources of F. Bach also states that because of peak times of traffic flow, among other variations during the day, the above proportioning has to be weighted according to the time of day. This supports the reasoning above that F generated by motor vehicles can be a major energy source during times of peak traffic flow, perhaps contributing much more than 1/3 of total F.

Rural cooling seems to follow a more normal pattern with maximum cooling at or shortly after sunset, again being more sensitive to variations in wind and cloud. The main differences evident under the calm and clear conditions of Figure 22b are that the maximum cooling is 0.5 $^{o}C\ hr^{-1}$ greater (at -1.5 $^{o}C\ hr^{-1}$) and the range of the oscillations of $\Delta T/\Delta t$ following this value is greater. This is a major contrast to the considerable greater maximum $\Delta T/\Delta t$ of -2.7 $^{o}C\ hr^{-1}$ in summer but the general pattern is similar. In general, $\Delta T/\Delta t$ seems to be more variable, especially in the rural area in the winter than in the summer.

The lack of any great difference in CBD and rural $\Delta T/\Delta t$ values for the general winter case accounts for the damped and irregular growth of heat island intensity (Figure 22a). The greater divergence of the rural cooling rate from that of the CBD on the calm clear nights gives rise to a more intense and regular build-up of ΔT_{u-r} (Figure 22b). Maximum ΔT_{u-r} occurs coincidentally with the maximum rural cooling rate, and the intensity stabilizes as urban and rural cooling rates approach the same value and remain in equilibrium for the remainder of the night.

c) Divergence of Cooling Rates

The rural area exhibits the expected values for nocturnal cooling rates and their progression through time, and it is in the urban area where the cooling rates have been modified. This divergence from the normal rural values can be attributed to the stored heat energy (G) and the artificial heat generation (F) within the urban area. As noted before, F generated by evening rush hour traffic and space heating appears to be the major source for the required extra urban heat in winter. In the summer, the major source is the portion of the previous day's Rn stored in the urban fabric (G).

Sufficient energy is added to the urban air from these sources at night to offset for the most part the radiational cooling process that acts almost equally (Oke and Fuggle 1971) in both the urban and rural areas. Fuggle (1971) reports that radiative cooling in Montreal is approximately three times as great as actual observed cooling ($\Delta T/\Delta t$) and concludes that nocturnal cooling in the lower urban atmosphere is driven by radiation with sensible heat transfer (H) acting as a retarding

influence. This is the essential contrast between the urban and rural areas, in that the rural cooling is also driven by radiation but without the retarding influence of the additional energy available in the urban area from G and F, and the resultant sensible heat transfer.

The result of the divergence of urban and rural $\Delta T/\Delta t$ is the development of a temperature difference between the two areas: the formation of the urban heat island.

3. Maximum ΔT_{u-r} and its Time of Occurrence

The previous section provided an explanation for the growth of the heat island over the night but only briefly mentioned maximum ΔT_{u-r} values during the night, and the time of occurrence of these maximum values. Some comments on these two aspects of the urban heat island seem necessary.

a) Maximum Nocturnal ΔT_{u-r} Values

The greatest heat island intensity observed during the observations for this study was 11.4 ^{o}C and occurred on the night of February 7-8, 1970 at 0500. This is very similar to extreme values reported for other cities in North America (Table 6). While a portion of other reported extreme intensities is probably attributable to topography and other non-urban controls in the cities concerned, it is felt that this is not the case in Montreal (Figure 7).

TABLE 6

Extreme Nocturnal Values of Heat Island Intensity

City	Date	ΔT_{u-r} (°C)	Author
Toronto, Ontario.	Feb. 22, 1936	16	Middleton and Millar (1936)
San Francisco, California.	Mar. 26. 1952	12	Duckworth and Sandberg (1954)
Edmonton, Alberta.	Feb. 11, 1963	11.5	Daniels (1965)
Montreal, Quebec.	Feb. 15, 1970	12	Oke and East (1971)

An intensity of 11.4 °C is probably not an unusual value for Montreal, however. On 11 of the 14 nights of all night observations the maximum intensity observed exceeded 9.0 °C, and was greater than 10.0 °C on 5 nights, as shown in Table 7 along with the mean wind and mean cloud for the hours between sunset and ΔT_{u-r} (max). Maximum intensities around 10.0 °C appear to be common in the Montreal area, and ΔT_{u-r} (max) on one of the summer nights (August 4-5) was 11.2 °C, indicating that maximum intensities can reach the same values in both summer and winter. These observations thus negate the conclusion of Oke and East (1971) that Montreal's heat island reaches its maximum intensity in winter.

However, their observation that there appears to be an upper limit of around 12 °C for heat island growth in temperate latitudes does have merit. When maximum heat island intensity is plotted against a

TABLE 7

Maximum Observed ΔT_{u-r} Values

Summer				Winter			
Date	ΔT_{u-r}(max) (^{o}C)	$\bar{u}$ (m sec^{-1})	$\bar{c}$ (tenths)	Date	ΔT_{u-r}(max) (^{o}C)	$\bar{u}$ (m sec^{-1})	$\bar{c}$ (tenths)
1970				1969			
July				Dec.			
23-24	9.9	1.5	0	16-17	5.0	1.4	0
24-25	10.3	0	0.2	17-18	7.3	2.5	0
27-28	5.5	2.5	0				
29-30	9.1	0	0.6	1970			
August				Feb.			
4-5	11.2	0.7	0.1	7-8	11.4	0.7	0.3
5-6	9.6	0.3	0.1	14-15	10.0	1.1	0.1
6-7	10.0	1.5	0				
7-8	9.5	1.8	0.2				
8-9	9.2	0.9	0.2				
9-10	9.5	0.3	0				

combination of mean wind and mean cloud from Table 7, a relationship is visible that supports their opinion (Figure 23). There are insufficient points on Figure 23 to calculate a valid regression line statistically, so the line shown was fitted by eye. This line intersects the abcissa of the diagram around $\Delta T_{u-r} = 11.5\ ^{o}C$. This is interpreted to mean that, as the mean wind and cloud between sunset and the time of maximum ΔT_{u-r} during the night simultaneously approach zero, maximum ΔT_{u-r} approaches 11.5 ^{o}C. Zero wind and zero cloud are the limiting 'ideal' weather conditions for heat island studies, so it can be said that around 11.5 ^{o}C is the upper limit for heat island growth in Montreal.

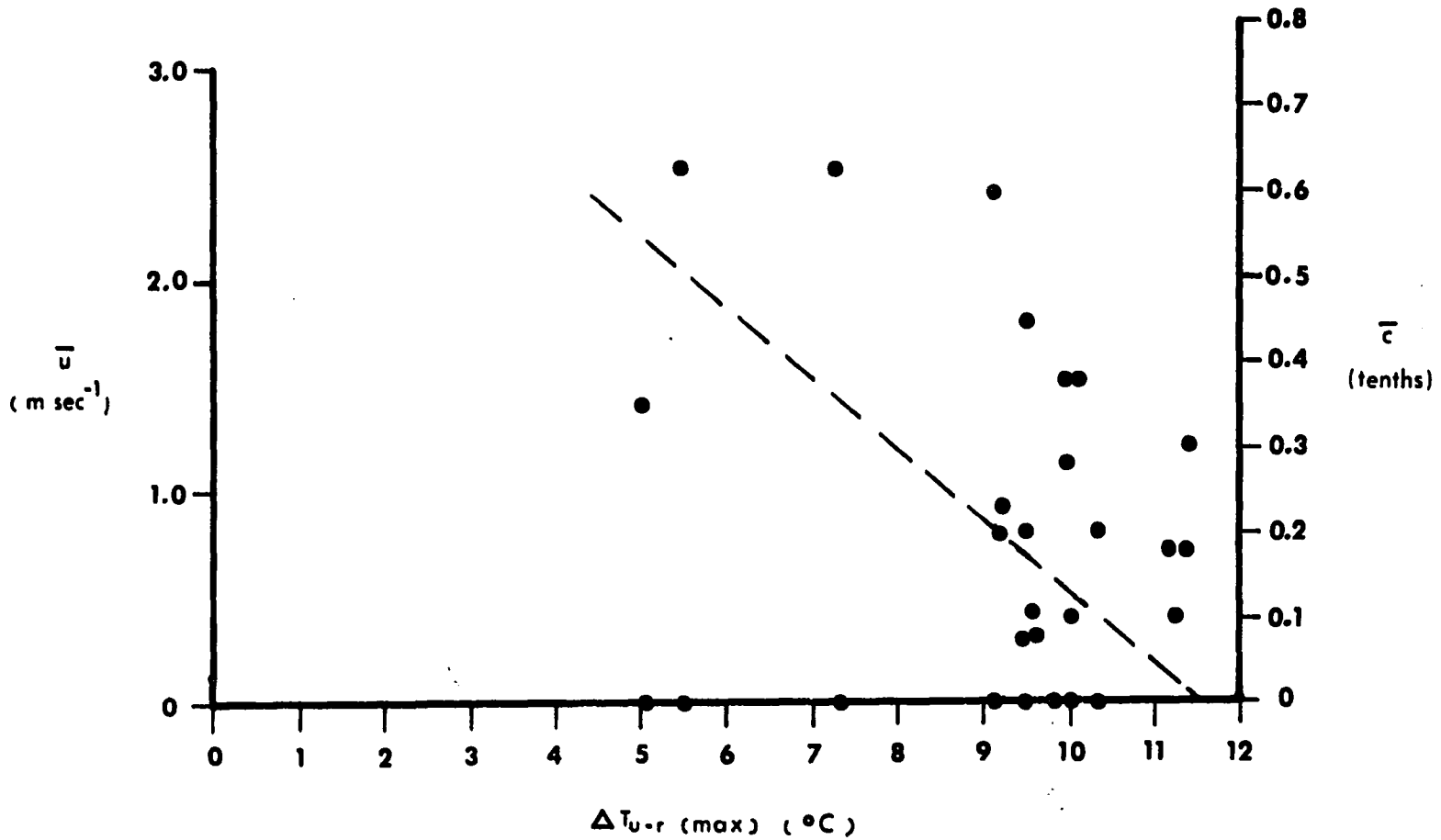

Figure 23: ΔT_{u-r}(max) vs. mean wind ($\bar{u}$) and mean cloud ($\bar{c}$) from sunset to time of ΔT_{u-r}(max). Summer and winter nights combined.

b) Time of Occurrence of Maximum Values

Table 8 shows the time interval[1] between sunset and maximum ΔT_{u-r} for selected observation nights. By only considering nights that were calm and clear for the period between sunset and the time of maximum ΔT_{u-r} it was possible to hold two of the controlling factors (wind and cloud) constant.

TABLE 8

Time Interval Between Sunset and ΔT_{u-r} max on Calm, Clear Nights

Date (1970)		ΔT_{u-r} max (^{o}C)	Time Interval (hours)
July	24 - 25	10.3	3
August	8 - 9	9.2	3
	9 - 10	9.5	4
February	14 - 15	10.0	5
August	4 - 5	11.2	6
	5 - 6	9.6	7

The nights of August 4-5 and 5-6 appear to be the abnormal ones with a 6 and 7 hour time interval respectively. However, Figure 24 shows that the maximum intensity was almost reached within 4 hours of sunset on both those nights. This seems to indicate that under ideal wind and cloud conditions in Montreal the maximum ΔT_{u-r} is normally reached between 3

1. Time taken to the nearest full hour.

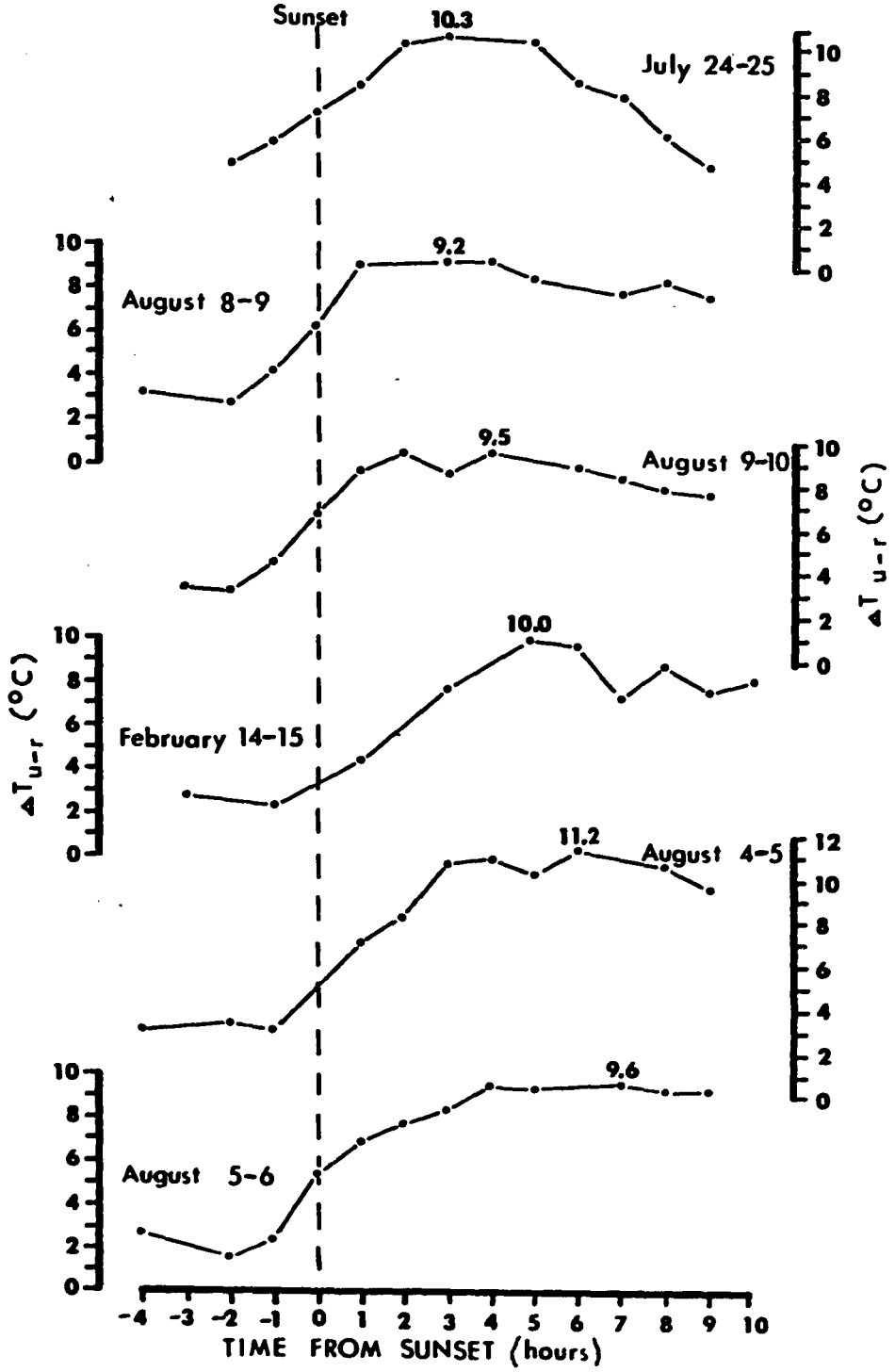

Figure 24: Build-up of ΔT_{u-r} on nights that were calm and clear between sunset and maximum ΔT_{u-r}. Maximum value of ΔT_{u-r} is given for each night.

and 4 hours after sunset.

This time lag is difficult to explain since the maximum rural cooling $\Delta T/\Delta t$ has been shown to occur at or around sunset and it is as a response to this extreme cooling that one would expect the extreme $\Delta T_{u-r}(max)$ to occur, possibly coincidentally. However, this three to four hour time lag may be the time required following the occurrence of maximum $\Delta T/\Delta t$ for the rural area to cool down to the point that the difference between rural temperatures and urban temperatures is at its maximum.

Numerous attempts were made to relate the time intervals in Table 8 to heat island intensity, cooling rates, and certain quantifiable factors that it was thought might explain the variation in time intervals, but no specific relationships could be defined. The same analyses were attempted for the remaining nights (Table 9) with as little success.

It is therefore concluded that it is the combination of all aspects of the urban and rural areas and the heat island that determine, under the control of wind and cloud, the actual time interval in each particular case. The particular mixture of conditions that are essentially unique each night will make understanding of time interval variations difficult.

TABLE 9

Time Interval Between Sunset and ΔT_{u-r}(max) on Nights with Scattered Cloud and Light Winds

Date	ΔT_{u-r} (max) (^{o}C)	Time Interval (hours)
July 27-28/70	5.5	4
July 29-30/70	9.1	5
Aug. 6-7 /70	10.0	5
Dec. 17-18/69	7.3	6
July 23-24/70	9.9	7
Aug. 7-8 /70	9.5	7
Feb. 7-8 /70	11.4	10
Dec. 16-17/69	5.0	12

CHAPTER VI

URBAN MORPHOLOGY AND AIR TEMPERATURES

This chapter provides observational evidence of the influence of changes in urban morphology on air temperatures in the Montreal area.

It was felt that a spatial averaging of temperature within each area of differing morphology would provide a more accurate and representative temperature value than one single observation, or series of observations however chosen. For this reason, a series of temperature observations were abstracted from the hourly traverse charts within the CBD, industrial, residential and rural sections of the traverse (Chapter III). These observations were then averaged to arrive at an 'area mean' temperature for each area and time series of hourly temperatures were developed for each night. By taking the spatial variation into account in this manner, the basic nature of the effects variations in fabric and structure from area to area have on air temperatures should be easily discernable.

Figures 25 to 29 show typical parts of the CBD, industrial, residential and rural areas and give an idea of the fabric and structure of the urban surface in each area.

The essential nature of the differences in temperature among the four areas is shown in Figure 30a & b for the night of August 9-10, 19 0.

The area mean temperatures in Figure 30a show that there is little difference between the CBD and industrial areas, and that they are

Figure 25: Central Business District (1).

Figure 25: Central Business District (1).

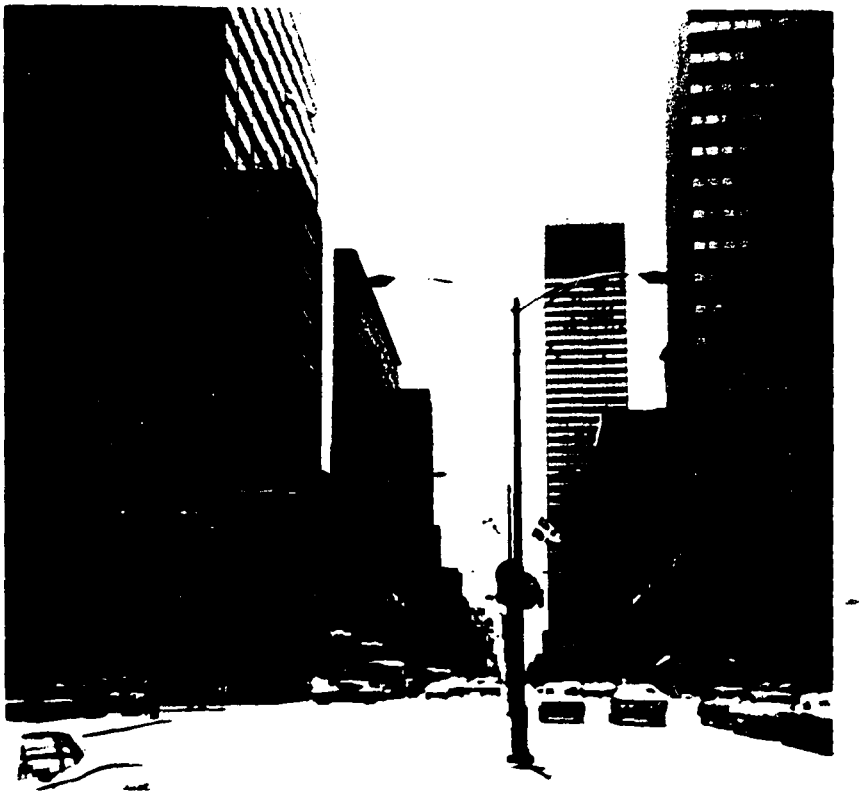

Figure 26: Central Business District (2).

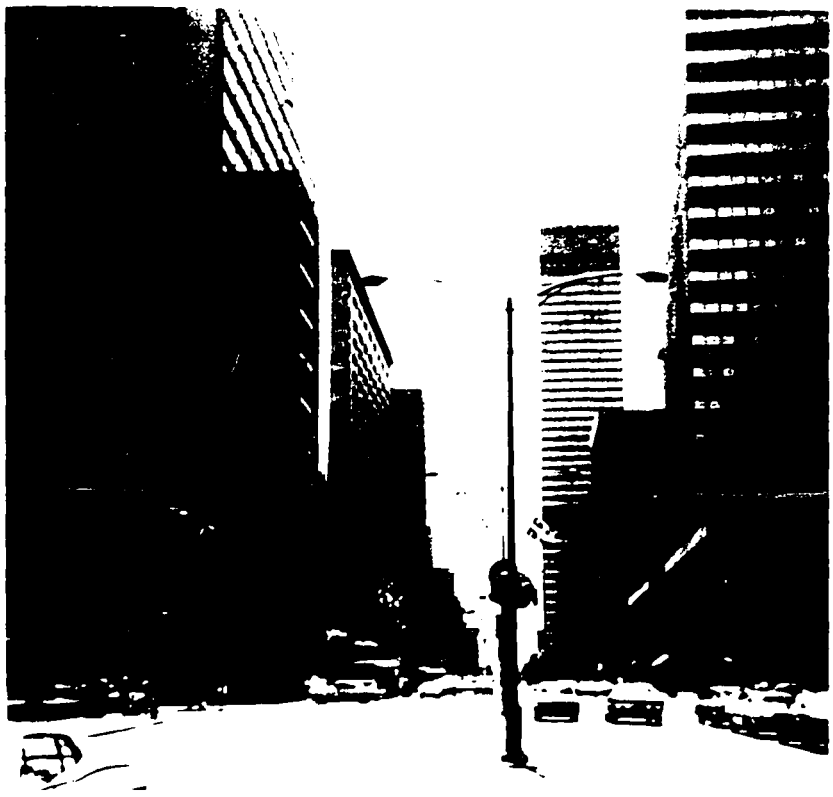

Figure 27: Industrial area.

Figure 28: Residential area.

Figure 27: Industrial area.

Figure 28: Residential area.

Figure 29: Rural area.

Figure 29: Rural area.

the warmest of the four areas. It is not surprising that there is little difference in temperature because, firstly, their structure and fabric are quite similar (a dense array of multistory buildings and an almost 100% asphalt, concrete and stone fabric). Secondly, these two areas are adjacent, thus any air circulation is bound to lead to interchange between them. In addition, the industrial area is adjacent to the river which has a moderating influence on temperatures there. The residential area with its more open structure and a greater proportion of vegetated area in its fabric is consistently about 1 ^{o}C cooler throughout the night. The rural area, by definition land in its natural vegetated state and not in close proximity to a densely urbanized area, is a further 1.5 ^{o}C cooler than the residential area.

It would appear that urban air temperature variations are related closely to changes in morphology as outlined here. Such changes in morphology have their strongest effect on the storage term (G) of the heat balance. It thus seems that G may be a more important term than previously thought and that temperature variations due to H, LE, and F operate superimposed on this basic relationship.

Figure 30b shows the cooling rates ($\Delta T/\Delta t$) in the four areas and the essential nature of the differences follows the same pattern as that for temperature. CBD and industrial areas exhibit the lowest cooling rates throughout the night mainly due to the thermal inertia of their structure and fabric which tends to oppose the nocturnal cooling evident in the rural $\Delta T/\Delta t$ curve. The residential area, because of its intermediate structure and fabric maintains intermediate values of cooling

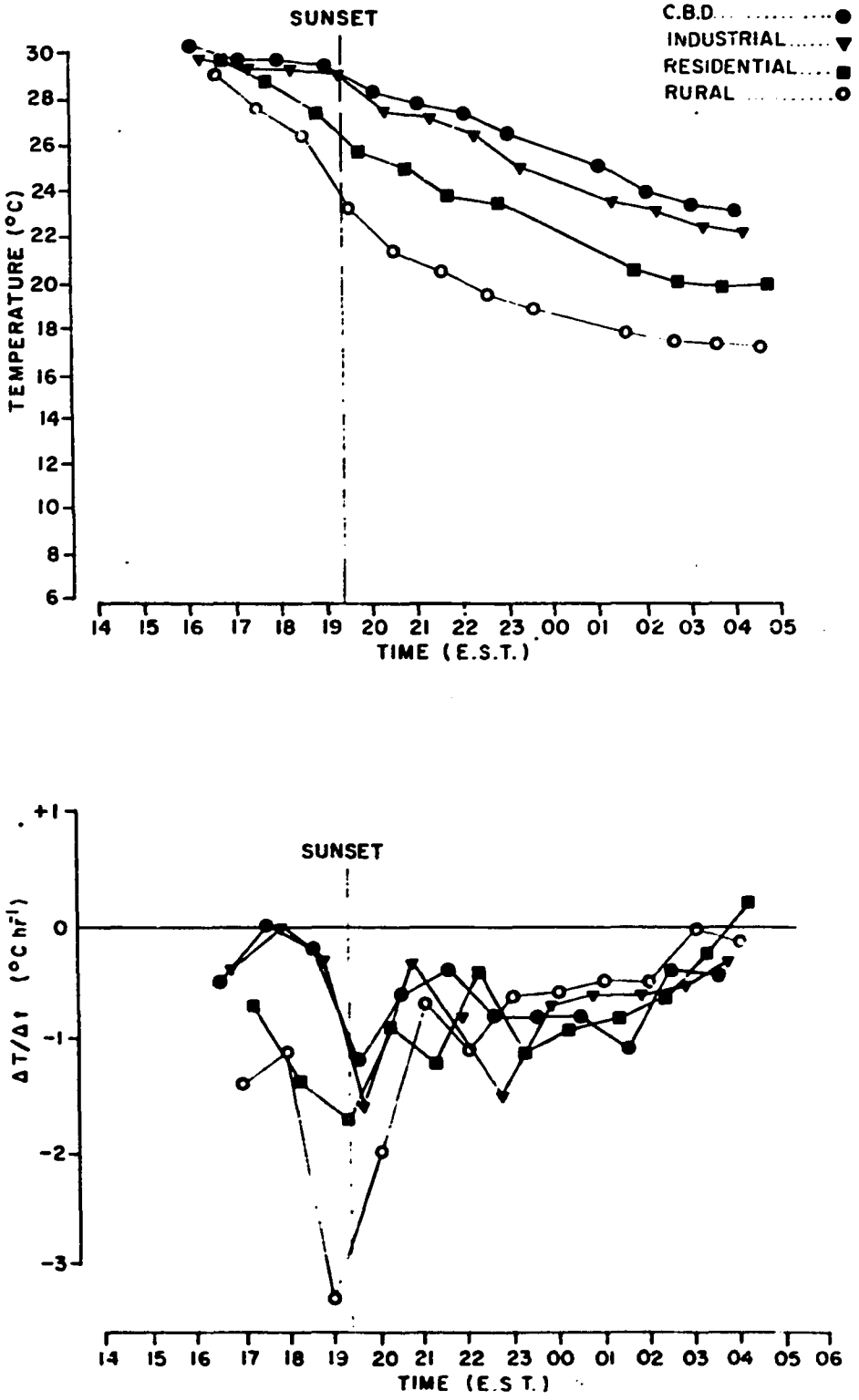

Figure 30: a) Air temperatures and b) cooling rates ($\Delta T/\Delta t$) by land use area for the night of August 9-10, 1970.

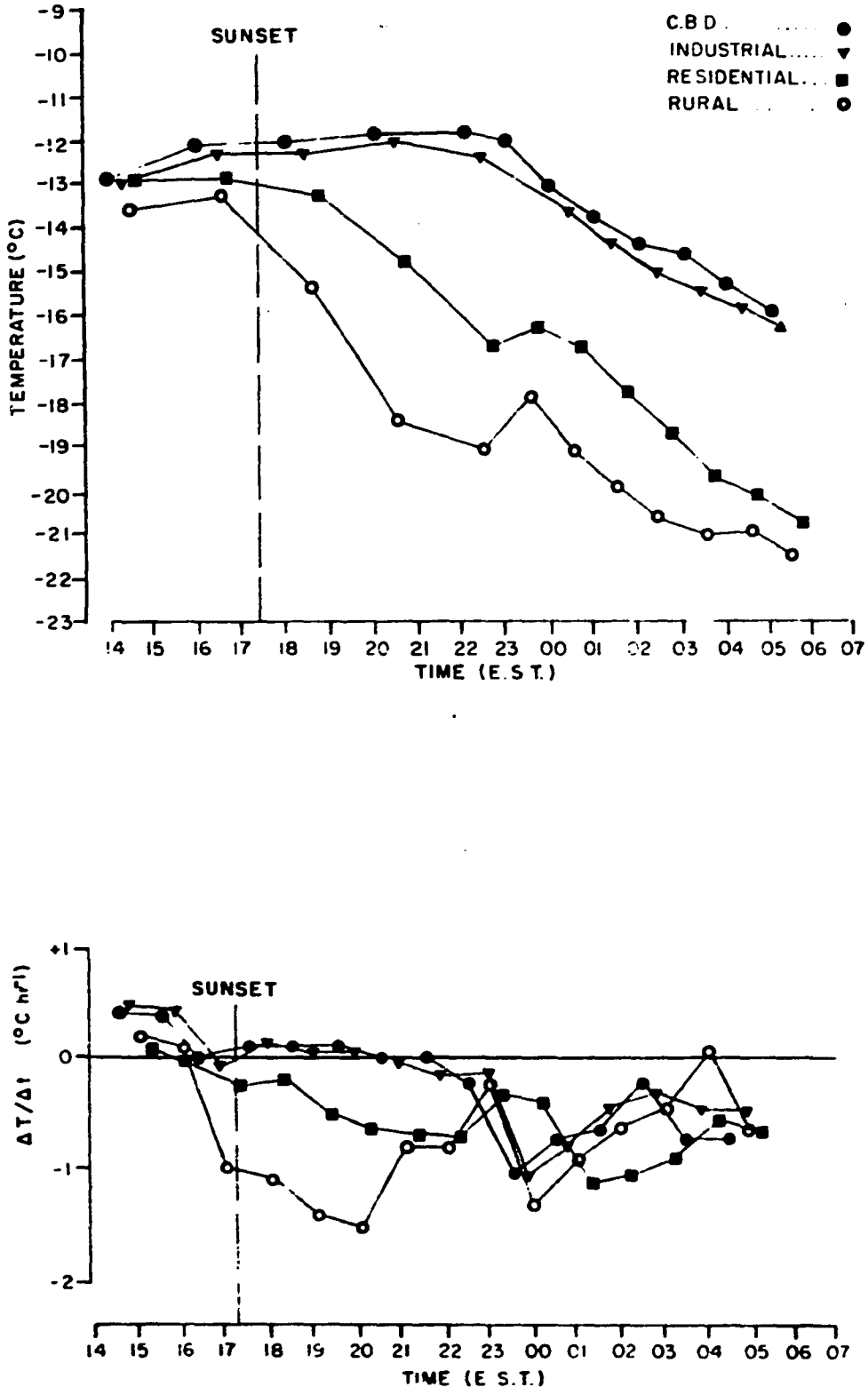

Figure 31: a) Air temperatures and b) cooling rates ($\Delta T/\Delta t$) by land use area for the night of February 14-15, 1970.

rates. Cooling rates in all four areas tend to equalize several hours after sunset as the rural $\Delta T/\Delta t$ decreases from its extreme values to approach that of the CBD. This has been discussed more fully in Chapter V.

Virtually the same pattern is shown in Figure 31a and b with the exception that the differences between the CBD/industrial, residential, and rural temperatures are greater on this winter night (Figure 31a), and the cooling rates take longer to equalize following sunset (Figure 31b). The major factor to account for these greater variations is the additional energy input from the artificial heat generation of space heating and other sources (F), which has been calculated to be 0.218 ly min^{-1} for Montreal in the winter (Oke 1969). The comparable value for summer is much smaller: 0.081 ly min^{-1}. This additional energy input also could account for the warming rates, rather than cooling, in the early part of the evening.

The above observations support statements by previous authors (Chapter I) concerning the major influence morphology has on urban air temperatures. However, Duckworth and Sandberg (1954) may be over generalizing when they state that morphology is the most important single factor in increasing the temperature in an urban area. This seems to be valid in summer but may be open to question in winter, due to the apparent major influence of artificial heat generation demonstrated above.

CHAPTER VII

SUMMARY OF CONCLUSIONS

1. Sampling Density

A selection of sampling densities comparable to those used in previous studies of the urban heat island were compared. A density of 1 point km^{-2} was found to be inadequate to depict urban air temperature patterns, even in the most generalized manner. Further analysis indicated that a density of 7 points km^{-2} is the optimum for use in a study in which the goal is to investigate the general pattern of urban air temperatures. This density shows the relation between air temperatures and the urban structure and fabric in considerable detail.

A detailed analysis of air temperature variations within the 23.7 km^2 study area confirmed certain influences of an urban area on air temperatures, and demonstrated certain aspects that have not been thoroughly investigated before due to inadequate sampling densities.

Firstly, cool air drainage off Mount Royal has an important influence in the particular area studied. Secondly, parks and open spaces are characterized by temperatures approximately 0.5 ^{o}C cooler than the surroundings. The cooling effect of parks and open spaces is already well known, and these observations have important implications for urban planners and architects who are concerned with the effects their planning and buildings might have on the urban climate. In general, cool air drainage such as this should be utilized to improve air circulation within the immediate area by the proper design and location of buildings

and streets.

Thirdly, a temperature range within the study area of 2.2 ^{o}C was observed indicating that temperature variations related to distinct land-uses within a small area of the city of Montreal are possible under favourable meteorological conditions.

Fourthly, there appears to be a distinct division of the study area into two temperature regimes with a noticable temperature 'cliff' dividing them. This division is related to the division of the study area in two parts by the band of industry along the C.P. Rail tracks. This break in the uniformity of structure and fabric within the area provides a natural boundary for a change in air temperature regimes, by itself or in combination with an external influence such as the cool air drainage from Mount Royal. An air flow such as this is likely to be channelled by a variation in the form and structure of the urban surface. Fifthly, main traffic arteries appear to give rise to distinct warm spots or tongues, as would be expected from the localized energy input in the form of the exhaust from motor vehicles and the concentration of human activity along such arteries.

Sixthly, maximum temperature gradients equivalent to the gradient of 5.0 ^{o}C km^{-1}, were observed and as such are greater than gradients that have been observed at the edge of the heat island. Since the thermal gradient at the edge of the heat island is known to generate thermal breezes these gradients are likely to generate thermal winds within the city itself. Such winds may be important in the dispersion of air pollutants, and the amelioration of block size microclimate by improving

air circulation.

2. Heat Island Intensity

Divergence of nocturnal cooling rates between urban and rural areas were shown to explain the development of the heat island. Urban cooling rates are held at low values through the retarding influence the additional heat energy available from F and G in the city has on nocturnal radiational cooling. This retarding influence does not act in the rural area.

Rural cooling rates were shown to attain their maximum values (up to -2.7 $^{o}C\ hr^{-1}$) at or shortly after sunset as would be expected; and then drop to the same values as the urban area (around -0.7 $^{o}C\ hr^{-1}$) for the remainder of the night. As a result, the heat island is formed for the most part in the early evening and then stabilizes between 7.0^{o}C and 8.0 ^{o}C for the remainder of the night after having attained its maximum value. This maximum was found to occur three to four hours after sunset, and to have a limiting value of 11.5 ^{o}C under ideal wind and cloud conditions. Intensities approaching this value were observed both in summer and winter, indicating that there is no seasonal differentiation in maximum nocturnal intensities. Typical nocturnal summer intensity values are around 8.0 ^{o}C and typical winter values are about 1.0 ^{o}C less.

3. Urban Morphology

Urban morphology was shown to have a major influence on urban air temperatures leading to the conclusion that the heat storage term (G)

of the nocturnal urban heat balance may be a more important term especially in summer than has been previously stated.

Air temperatures and cooling rates were shown to differ as a result of variations of fabric and structure with changes in land use. The residential area is consistently at least 1.0 ^{o}C cooler than the CBD and the rural area consistently a further 1.5 ^{o}C or more cooler.

One implication of the variation in cooling rates within the urban area is that the standard method of correcting temperature traverse observations to a common time for analysis may not be as good an approximation to the true correction required as has been thought. The error of closure technique, if based on one closure point, assumes that the change in temperature at that point is representative of temperature changes throughout the traversed area. If the traverse passes through areas of different land use, and thus differing morphology, the resultant variations in cooling rates demonstrated in this thesis indicate that temperature change at one point does not represent temperature change in the whole urban area. A closure point within the urban area certainly does not represent temperature change in a rural area. A correction technique that utilizes several closure points in the land use areas traversed or a correction factor that differentiates among land uses is necessary.

BIBLIOGRAPHY

Bach, W. (1970), An Urban Circulation Model, Arch. Met. Geoph. Biokl., Ser. B., 18, 155-168.

Bornstein, R.D. (1968), Observations of the Urban Heat Island Effect in New York City, J. App. Meteorol., 7, 575-582.

Chandler, T.J. (1961), Surface Breeze Effects of Leicester's Heat Island, East-Midland Geographer, 15, 32-38.

Chandler, T.J. (1962a), Temperature and Humidity Traverses Across London, Weather, 17, 235-242.

Chandler, T.J. (1962b), Diurnal, Seasonal and Annual Changes in the Intensity of London's Heat Island, Met. Mag., 91, 146-153.

Chandler, T.J.,(1965), The Climate of London, Hutchinson & Co., London, 292 p.

Chandler, T.J. (1970), Urban Climates: Inventory and Prospect. Proc. WMO Symposium on Urban Climates and Building Climatology, 1968. Vol. 1, Urban Climates. WMO Tech. Note 108, 1-14.

Daniels, P.A. (1965), The Urban Heat Island and Air Pollution with Application to Edmonton, Alberta. (Unpublished M.Sc. Thesis, Dept. of Geography, University of Alberta, Edmonton).

Delage, Y. and P.A. Taylor (1970), Numerical Studies of Heat Island Circulations, Boundary Layer Meteorology, 1, (2), 201-226.

Duckworth, F.S. and J.S. Sandberg (1954), The Effect of Cities Upon Horizontal and Vertical Temperature Gradients. Bull. Amer. Meteorol. Soc., 35, 198-207.

Fuggle, R.F. (1968), Preliminary Thoughts on Long Wave Radiation Flux Divergence and the Urban Heat Island, Climatological Bulletin, McGill University, (4), 31-39.

Fuggle, R.F. (1971), Nocturnal Atmospheric Infrared Radiation in Montreal, Unpublished Ph.D. Thesis, Dept. of Geography, McGill University, Montreal, 237 p.

Garnett, A. and W. Bach (1965), An Estimate of the Ratio of Artificial Heat Generation to Natural Radiation Heat in Sheffield. Monthly Weather Review, 93, 383-385.

Garnett, A. and W. Bach (1966), An Investigation of Urban Temperature Variations by Traverses in Sheffield. Biomet. II, 601-607.

Geiger, Rudolf, (1965), The Climate Near the Ground (Revised)(Translation) Harvard University Press, Cambridge, Mass., 611 p.

Godin, J. (1969), Variations de la temperature diurne a l'observatiore McGill, (thèse de maitrise présentée au dépt. de meteorologie, de l'université McGill.)

Gold, E. (1956), Smog: The Rate of Influx of Surrounding Cleaner Air, Weather, 11, (7), 230-232.

Hutcheon, et al (1967), Observations of the Heat Island in a Small City Bull. Amer. Meteorol. Soc., 48, 7-9.

Kraus, E. (1945), Climate Made by Man, Quart J. Roy. Meteorol. Soc. 71, 397-412.

Landsberg, H.E. (1956), The Climate of Towns in Mans Role in Changing the Face of the Earth, edited by William L. Thomas, Jr., University of Chicago Press, Chicago, 584-606.

Landsberg, H.E. (1958), Physical Climatology - 2nd Revised Edition Gray Printing Co., DuBois, Penn, 446 p.

Lindquist, Sven (1968), Studies on the Local Climate in Lund and its Environs, Geografiska Annaler, 50(A), (2), 79-93.

Lowry, W.P. (1967), The Climate of Cities, Scientific American 217, (2), 15-23.

Ludwig, F.L. (1967), Urban Climatological Studies, (Interim Report No. 1) Stanford Research Institute Project, #MU-4945-580, 97p.

Ludwig, F.L. (1969), Personal Communication.

Ludwig, F.L. and J.H.S. Kealoha (1968), Urban Climatological Studies (Final Report) Stanford Research Institute Project # MU-6300-140.

Middleton, W.E.K. and F.G. Millar (1936), Temperature Profiles in Toronto Royal Ast. Soc. (Tor.) J., 30: 265-272.

Mitchell, J.M. (Jr.) (1953), On the Causes of Instrumentally Observed Secular Temperature Trends, J. Meteorol., 10(4), 244-261.

Munn, R.E. (1966), Descriptive Micrometeorology, Advances in Geophysics, Supplement 1, Academic Press, New York, 245p.

Oke, T.R. (1968), Some Results of a Pilot Study of the Urban Climate of Montreal, Climatological Bulletin, McGill University, (3), 36-41.

Oke, T.R. (1969), Towards a More Rational Understanding of the Urban Heat Island, Climatological Bulletin, McGill University, (5), 1-20.

Oke, T.R. and F.G. Hannell (1970), The Form of the Urban Heat Island in Hamilton, Canada. Proc. WMO Symposium on Urban Climates and Building Climatology, 1968. Vol. 1, Urban Climates. WMO Tech. Note 108, 113-126.

Oke, T.R. and C. East (1971), The Urban Boundary Layer in Montreal, Boundary Layer Meteorology 1, 411-437.

Oke, T.R. and R.F. Fuggle (1971), Comparison of Urban/Rural Counter and Net Radiation at Night, Boundary Layer Meteorology, (In Press).

Peterson, J.T. (1969), The Climate of Cities: A Survey of Recent Literature. U.S. Dept. Health, Educ. Welfare; Public Health Service; Consumer Protection and Environmental Health Service, National Air Pollution Control Administration, Raleigh, North Carolina, 48 p.

Powe, N.N. (1969), The Climate of Montreal, Climatological Studies 15, Meteorological Branch, Dept. of Transport, Toronto, 51p.

Sekiguti, T. (1964a), The Distribution of Winter Time City Temperature in and Around Yonezawa in Northern Japan, Tokyo J. Climatology, 1(1), 13-16.

Sekiguti, T. (1964b), City Climate Distribution in and Around Ogaki, A Medium Sized City in Central Japan, Tokyo, J. Climatology, 1(1), 17-28.

Sundborg, A (1950), Local Climatological Studies of the Temperature Conditions in an Urban Area. Tellus 2(3), 221-231.

Sundborg, A. (1951), Climatological Studies in Uppsala with Special Regard to the Temperature Conditions in the Urban Area. Geographica 22, Geographical Institute, University of Uppsala, Uppsala, 111p.

Summers, P.W. (1964), An Urban Ventilation Model Applied to Montreal, Unpublished Ph.D. Thesis, Dept. of Meteorology, McGill University, Montreal.

Yap, D. (1969), Air Pollution and Vertical Temperature Distribution over Montreal. Unpublished M.Sc. Thesis, Dept. of Meteorology, McGill University, Montreal.

Yap, D., K.L. Gunn and C. East (1969), Vertical Temperature Distribution over Montreal, Naturaliste Can., 96, 561-580.

APPENDIX I

WEATHER CONDITIONS AND OTHER DATA FOR OBSERVATION NIGHTS

	PREVIOUS DAY'S								
	1	2	3	4	5 WIND			6 CLOUD			7
NIGHT of	SUNSET	TIME OF LAST SUN	Q . q (ly)	SYNOPTIC	Times	Direction	Speed ($m\ sec^{-1}$)	Times	Amount (tenths)	Type	SNOW ON GROUND (cm)
1969											
November 27 - 28	1615	1520	162	Temperatures below normal.	1400-0700	Calm		1400-0800	Clear		5
December 16 - 17	1612	1430	128	Seasonable temperatures. Light snow showers in early morning (16th).	2000-2300 0000-0800	Calm S/SW	1.8-3.6	1400-0800	Clear		tr
December 17 - 18	1612	1100	68	Seasonable temperatures. Light snow in morning and early afternoon (17th).	2000-0200 0300-0800	Calm to W/WNW Calm	3.1	1400-0800	Clear		tr
1970											
February 7 - 8	1709	1535	141	Mainly cloudy becoming mainly sunny by late morning. Mild.	1400-0800	Calm		1400-0100 0200-0400 0500-0800	Clear to 0.7 Clear Fog	AcCi	43
February 14 - 15	1720	1610	292	Mainly sunny and cold.	1400-1800 1900-0500 0600-0800	W/WSW/SW Calm N	1.8-6.3 4.0-5.4	1400-0400 0500-0700	Clear 0.4-0.6	Ci	41
March 30 - 31	1819	1720	468	Mainly sunny and cold.	1400-1500 1600-0200 0300-0800	Calm NE Calm	1.8-4.5	1400-1700 1800-0800	0.5-0.6 Clear	CiCs	13
March 31 - April 1	1821	1705	457	Mainly sunny with seasonable temperatures.	1400-0100	WSW/SW	1.8-4.0	1400-0800	Clear		13
May 14 - 15	1917	1755	659	Mainly sunny with seasonable temperatures.	1500-0600	Calm to NE	4.9	1400-0700	Clear except: 1700-2000 0.4-0.6 Ci 0400-0600 0.4-0.9 AcCi		--
May 18 - 19	1921	1830	549	Mainly sunny with seasonable temperatures.	1400-1800 1900-0300 0400-0700	Calm Calm to S/SW Calm	2.7	1400-1700 1800-0700	0.6-0.9 Clear	CFAcCi	--
May 28 - 29	1932	1850	712	Sunny with temperatures below normal.	1400-2000 2100-0700	SW/WSW Clear	1.8-3.6	1400-0700	Clear		--

APPENDIX I (cont'd)

	PREVIOUS DAY'S										
	1	2	3	4	5 WIND			6 CLOUD			7
NIGHT of	SUNSET	TIME OF LAST SUN	Q • q (ly)	SYNOPTIC	Times	Direction	Speed (m sec^{-1})	Times	Amount (tenths)	Type	SNOW ON GROUND (cm)
May 30 - 31	1934	1850	656	Sunny with maximum temperature well above normal.	1400-0700	S/SW	1.8-7.2	1400-1600 1700-0300 0400-0700	0.5-0.8 Clear 0.9-1.0	Ci ScAc	--
June 25 - 26	1947	1900	589	Overcast with rainshowers in early morning, becoming mainly sunny by mid-morning. Moderate southwesterlies in early morning.	1400-1800 1900-2300 0000-0700	W/WNW W Calm	4.9-7.6 2.7-4.5	1400-2100 2200-0700	0.2-0.4 Clear	Cu	--
June 28 - 29	1947	1855	727	Sunny with temperatures below normal.	1400-1900 2000-0100 0200-0700	SW/WSW SW Calm to S 3.6	4.5-6.7 2.2-4.5	1400-0300 0400-0700	Clear 0.5-0.6	 AcCi	--
July 23 - 24	1933	1835	643	Sunny and very warm. Moderate westerly winds in early morning.	1400-2300 0000-0700	SW/WSW Calm	1.8-5.4	1400-0700	Clear		--
July 24 - 25	1932	1810	625	Sunny and very hot. Record maximum temperature for this date.	1400-1700 1800-0200 0300-0700	SW Calm SE	1.8-4.0 1.8-2.2	1400-1600 1700-2000 2100-0000 0100-0600	Clear 0.5-0.8 Clear 0.6-0.9	 Ci CiAc	--
July 26 - 27	1930	1830	540	Sunny, hot, humid.	1400-1900 2000-0700	WSW/SW WSW/SW	6.7-7.6 1.3-4.9	1400-1700 1800-0000 0100-0300 0400-0700	0.3-0.6 0.2-0.6 Haze 0.4-0.5	Cuci Ac, haze AcCi, fog, haze	--
July 27 - 28	1929	1830	555	Mainly sunny, very hot and humid.	1400-0700	WSW/SW/S	1.8-7.2	1400-1800 1900-0100 0200-0400 0500-0700	0.2-0.4 Haze Fog 0.8	CuCi AcCi, fog	
July 28 - 29	1928	1810	385	Mainly cloudy with light rain and thundershowers in the late afternoon. Hot and very humid.	1400-1600 1700-2300 0000-0700	SW SW Calm	4.9-6.7 1.8-4.0	1400-1800 1900-0000 0100-0700	0.7-0.9 Clear Fog	CuAcCi	--
July 29 - 30	1927	1730	365	Partly cloudy with light rainshowers in the early afternoon. Very hot and humid.	1400-0700		Calm	1400-0000 0100-0400 0500-0700	0.6-1.0 Clear 0.6-0.8	CuCi AcCi, fog	--
August 4 - 5	1919	1825	n/a* •	Mainly sunny with maximum below normal.	1400-2000 2100-0400 0500-0700	Calm to NW 7.2 Calm SE	 1.8-2.2	1400-1900 2000-0700	0.4-0.5 Clear	CuCi	--
August 5 - 6	1917	1825	n/a	Sunny with seasonable temperatures.	1400-2000 2100-0700	W/SW Calm	2.2-5.4	1400-0700	Clear		--
August 6 - 7	1916	1825	n/a	Sunny with seasonable temperatures.	1400-2200 2300-0200 0300-0700	SW Calm S	2.2-5.4 1.8-2.2	1400-0700	Clear		--

APPENDIX I (cont'd)

	PREVIOUS DAY'S									
	1	2	3	4	5 WIND			6 CLOUD			7
NIGHT of	SUNSET	TIME OF LAST SUN	Q . q (ly)	SYNOPTIC	Times	Direction	Speed ($m\ sec^{-1}$)	Times	Amount (tenths)	Type	SNOW ON GROUND (cm)
August 7 - 8	1915	1805	n/a	Sunny and warm.	1400-0000 0100-0200 0300-0400 0500-0700	SW Calm SSW Calm	1.8-4.5 2.2 	1400-1700 1800-2100 2200-0400 0400-0700	0.2-0.6 0.3-0.7 	CuCi CuAcCi Clear Fog	--
August 8 - 9	1913	1820	n/a	Sunny and hot.	1400-1900 2000-0100 0200-0700	SW Calm S/SE	1.8-5.4 1.8-2.7	1400-2000 2100-0400 0500-0700	0.3-0.5 0.3	CuCi Clear AcCi fog	--
August 9 - 10	1912	1810	n/a	Mainly sunny and hot.	1400-0700	Calm		1400-0700		Clear	--
August 13 - 14	1906	1800	n/a	Mainly sunny, very hot and humid.	1400-1900 2000-0700	SW/WSW SW/SSW	4.5-6.7 1.8-3.6	1400-0300 0400-0700	 0.3-0.4	Clear AcCi	--
August 14 - 15	1904	1810	n/a	Sunny, hot and humid.	1400-0700	SW/WSW	2.2-7.2	1400-0700		Clear	--
August 31 - Sept. 1	1835	1750	n/a	Mainly sunny by mid-morning. Cool.	1400-0700	W/WNW	4.0-9.4	1400-1900 2000-2200 2300-0700	0.1-0.3 0.1-0.7	CF Clear ScAc	-

SOURCES:

1. Canada National Research Council, Division of Physics, Table of Sunrise and Sunset Times for Montreal, Quebec, 1970.
2. McGill Observatory Official Weather Abstracts. Time at which the last sunshine was observed at the Observatory.
3. Canada, Ministry of Transport, Meteorological Service Monthly Radiation Summaries. Global solar radiation received within the City of Montreal (College Jean Brebeuf).
4. McGill Observatory Official Weather Abstracts.
5. Hourly Aviation Reports, St. Hubert airport.
6. Hourly Aviation Reports, St. Hubert airport.
7. McGill Observatory Official Weather Abstracts.

* All times are Eastern Standard Time.

** Not available. Instrument malfunction.